Extraction of Bio-Butanol using Supercritical Carbon Dioxide

A Major Qualifying Project
submitted to the faculty of
the Chemical Engineering Department at
WORCESTER POLYTECHNIC INSTITUTE
in partial fulfillment of the requirements for the
degree of Bachelor of Science.

Submitted by:

Chelsea Conlon

David Knutson

Mark Overdevest

Allison Rivard

Professor Michael Timko, Advisor

Associate Professor Geoffrey Tompsett

Abstract

Renewable biofuels such as butanol are being researched due to the continued depletion of fossil fuels. Researchers at MIT have recently discovered a *B. Megaterium* bacteria that survives under high pressure and anaerobic conditions. They are genetically manipulating the bacteria to produce biofuels such as butanol. Butanol is potentially a great alternative for the ethanol dominated biofuel market since it is more energy dense and less flammable than ethanol. At WPI we are operating a supercritical carbon dioxide extraction system compatible with the organism. Throughout the course of our project our team made many improvements to the system set up and procedure for operation. This paper focuses on the extraction results, trends, and models that were generated when operating the high-pressure extraction system. Overall the system showed a slight increase in the extraction rate when the initial butanol concentration was increased from 1 wt.% to 3 wt.% and when the flow rate of $scCO_2$ was increased. On the other hand, no change in the extraction rate was observed when the pressure of the system was varied from 1500 PSI to 2000 PSI. With the experimental data our team concluded that the extraction unit can extract about 80-85% of butanol in the first 30 minutes. In order to further the future research of this project, experimental and theoretical models were created. The models allowed us to predict extraction rates and overall mass transfer coefficients for runs that were not completed. Therefore, the models reduce the amount of experimental runs that need to be performed.

Table of Contents

Acknowledgements

We gratefully acknowledge funding from DOE grant: DE-SC0012555 6930635. We also would like to thank our collaborators at MIT, both the students and professors that helped begin and continue this project. Lastly, and most importantly, we would like to thank our advisors Professor Timko and Professor Tompsett and those in the WPI Chemical Engineering department especially Luke Jackson and Alex Maag.

Table of Figures

Table of Tables

Chapter 1: Introduction

Energy is important to society for everyday tasks and processes. Non-renewable carbon fuels, such as oil and coal, are most commonly used for the production of energy (Odell, 1999). Finding energy alternatives to fossil fuels is a growing need due to their global depletion and negative environmental impacts (Qureshi, 2010). An increasing alternative to fossil fuels are biofuels. Biofuels are an energy source created from renewable organic material (Odell, 1999). Burning biofuels is favorable to fossil fuels because they are considered carbon cycle neutral ("Carbon cycle 2.0," ND). Biofuels can come from many different organic materials like corn crops, leftover organic waste, algae, and other microorganisms (Qureshi, 2010). Currently, the main biofuels being produced or developed to substitute fossil fuels are ethanol, butanol, hydrogen and biodiesel (Fortman et al., 2008).

Chemical engineers have an important role in the development of biofuels. In addition to researching innovative processes to make biofuels, testing the feasibility of up scaling a process for commercial use is vital for future application. Determining if large-scale production is possible begins with modeling the behavior and energy outputs of the reaction and separation processes using various simulation programs. The next steps involve collecting experimental data and developing models to predict trends. These trends can help to evaluate the feasibility of upscaling the bench scale reactor. Adjusting and changing the process on a small scale is easier and important to complete before carefully scaling up the process to a pilot plant and eventually a full scale manufacturing plant.

Currently, ethanol is the most widely used biofuel, as it is economically feasible to manufacture on a large scale and easily produced through fermenting corn or other crops ("Ethanol as a Transportation Fuel," ND). Legislation is trying to increase the amount of ethanol in gasoline from the current 10% to further reduce harmful carbon emissions ("Ethanol as a Transportation Fuel," ND). However, ethanol might not be the most effective option since it is less economical to create than gasoline from petroleum and stores less available energy (Qureshi, 2010). Tax breaks have been implemented on ethanol manufacturing to incentivize industry production, yet it is still less lucrative than creating gasoline ("Ethanol as a Transportation Fuel," ND). Other biofuel options can potentially

provide more energy; butanol contains 30% more energy per volume than ethanol(Qureshi, 2010). For these reasons, other biofuels might be have potential a more practical alternative.

Butanol is a logical substitute because it stores more potential energy and has similar properties to ethanol (Qureshi, 2010). In addition, butanol's lower flammability makes it safer and its chemical properties make it easier to mix in any proportion with gasoline (Qureshi, 2010). This creates the potential for new fuel mixtures to be developed. Unfortunately, a major drawback is the difficulty to economically produce butanol on a large enough scale for the fuel industry (Ezeji, Qureshi, & Blaschek, 2007). The production of butanol through using organisms and microorganisms is a developing field (Qureshi, 2010). Research has started on genetically modifying organisms to produce butanol (Thompson, Prather, & Timko, 2014). However, the organism, *B.megaterium,* begins to self-inhibit at high concentrations of butanol and poisons itself (Thompson et al., 2014).

B.megaterium, an alcohol-producing organism that can survive under extreme pressure and supercritical conditions in an anaerobic environment, was recently recovered in a deep subsurface $scCO_2$ well (Thompson et al., 2014). It is rare for an organism to survive under those conditions. Researchers at MIT are currently in the process of genetically modifying that organism to produce butanol via a mechanism with a butanal intermediate (Thompson et al., 2014). Under those extreme conditions there are fewer competing chemical reactions and supercritical extraction can be utilized for collecting butanol (Thompson et al., 2014). This creates the potential to overcome some of the difficulties that come with creating and collecting butanol from biomass (Ezeji et al., 2007).

Our project focused on testing the bio-reactor, in a semi-batch mode using model aqueous-alcohol solutions. We extracted butanol from an aqueous solution using supercritical carbon dioxide. An experimental model for the system was generated from Tai and Wu's (2005) mass transfer model. The experimental data collected was used in the experimental model to calculate the mass transfer coefficient (K_la), which was then substituted back into the model to predict extraction result data. The effects of changing the initial concentration of butanol, system pressure, and mass flow rate of supercritical carbon dioxide on the mass transfer coefficient were determined through analyzing data using the experimental model. The experimental K_la was validated through using a

theoretical model generated from correlations for the mass transfer coefficient (K_l) and interfacial area (a). The correspondence between the experimental data and predicted behavior is important to validate current and future experiments. Previous and generic models did not result in accurate predictions of the available experimental data (Worrest, Fletcher, & Timko, 2015). Our experimental model can be used to predict the mass transfer rate of butanol in our system for future testing under different conditions.

Chapter 2: Background

2.1 Biofuels in the United States

2.1.1 Energy Consumption in the United States

A variety of fuels power every part of modern day life such as transportation, electricity, heating and cooling. Petroleum, natural gas and coal are the three main fossil fuels dominated energy consumption in the US for more than a century ("Energy Explained," 2015). In 2014 these three sources accounted for 81% of energy consumed ("Energy Explained," 2015). Fossil fuels and nuclear electric power are considered non-renewable ("Energy Explained," 2015). Non-renewable is defined as a source of energy that is finite and cannot be replenished in a short period of time ("Energy Explained," 2015). On the other hand, renewable means an energy source that can be regenerated ("Energy Explained," 2015). In recent years there has been a push to use renewable energy instead of non-renewable energy (Earley & McKeown, 2009). Although renewable energy made up only 10% of energy consumption in the US in 2014, the production and use of biofuels and non hydroelectric renewable sources doubled from 2000 to 2014 ("Energy Explained," 2015). In Figure 2.1, a pie chart breaks down the US energy consumption in 2014 by energy source ("Energy Explained," 2015).

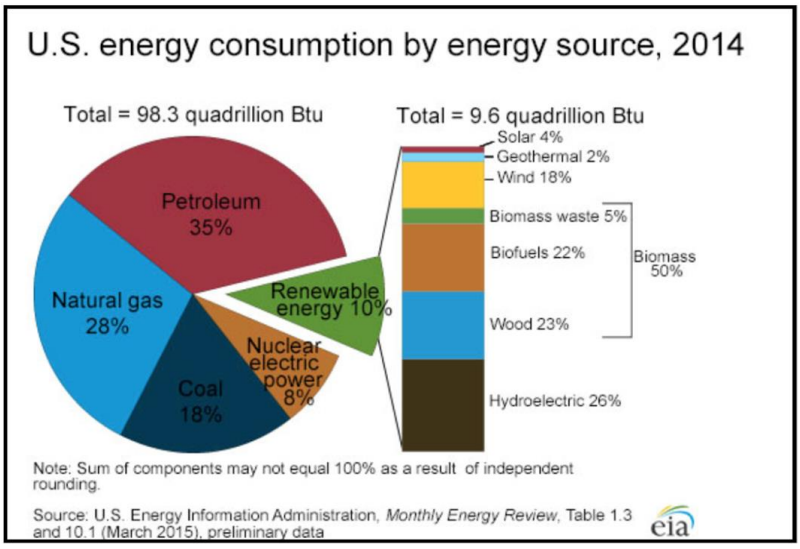

Figure 2.1: Energy consumption in the USA by energy source in 2014

2.1.2 Non-renewable and Renewable Energy Sources

Non-renewable energies, such as fossil fuels, are the most common source of energy consumed in the United States due to their abundance and low cost ("Energy Explained," 2015). However, there are a few major disadvantages to using fossil fuels such as a dependence on foreign oil and their contribution to climate change (Earley & McKeown, 2009). The United States government is fostering the production of renewable energy sources through laws and incentive programs, with goals to reduce greenhouse gas emissions and increase domestic energy production ("Energy Explained," 2015). The U.S's goal to reduce greenhouse gas emissions can be reached if the growth of renewable energy production continues (Earley & McKeown, 2009). Currently, the main challenge facing renewable energy is the high cost of production (Earley & McKeown, 2009). To overcome this, technological advances are needed to increase cost effectiveness of production (Earley & McKeown, 2009). With the push of government and society to reduce greenhouse gases there is an expected increase in renewable energy sources for the next 25 years ("Energy Explained," 2015).

2.1.3 US Government Support of Biofuels

Biofuels are one renewable energy option that the government currently supports (Earley & McKeown, 2009). The US biofuel industry started in the late 1990's to find a less toxic additive than MTBE (methyl tertiary butyl ether) for gasoline (Earley & McKeown, 2009). Following this, the agriculture sector lobbied the US for policies to increase US biofuel production to stimulate rural development and increase the demand and price of crops (Earley & McKeown, 2009). Today the Renewable Fuel Standard (RFS) is a law through which the US government supports biofuels through a variety of federal and state incentives (Earley & McKeown, 2009). This law calls for the blending of 36 billion gallons of biofuels annually into conventional motor fuels by 2022 (Earley & McKeown, 2009) . Additionally, individual state governments have passed laws that require a certain percentage of biofuel in each gallon of gasoline (Earley & McKeown, 2009). For example, Florida passed a law in 2008 that requires all gasoline sold in the state to contain 9-10% ethanol by 2010 (Earley & McKeown, 2009).

2.1.4 Advantages and Disadvantages of the Most Common Types of Biofuels

Biofuels refer to a form of bioenergy derived from biological plant or animal matter, "biomass" (Earley & McKeown, 2009). A few examples of biofuels include: biodiesel, corn based ethanol, cellulosic ethanol, bio-butanol, biogas etc (Earley & McKeown, 2009). Ethanol is by far the most significant biofuel in the US making up 94% of biofuel production ("Biobutanol," 2015). The remaining 6% of biofuels mostly consists of biodiesel ("Biobutanol," 2015). Although the biofuel industry has grown tremendously throughout the past decade, there is still room for improvement. The disadvantages to using ethanol include increased food prices, large releases of carbon through land clearing, crop growth for food vs fuel, and stress on agricultural sectors that rely on corn for feedstocks (Earley & McKeown, 2009). Nearly all studies on biofuels found minimal reductions in greenhouse gas emissions using corn ethanol over gasoline (Earley & McKeown, 2009). In order for the use and sustainability of biofuels to increase in the future, it is necessary to move towards advanced biofuels (Earley & McKeown, 2009). Advanced biofuels come from non-food feedstocks and offer improved energy and greenhouse gas profiles over conventional biofuels (Earley & McKeown, 2009).

2.1.5 A Comparison of Butanol and Ethanol

While ethanol is today's most common biofuel there are many other possibilities, one of which is butanol ("Carbon cycle 2.0," ND). In Figure 2.2 you can find a chart comparing the fuel properties of gasoline, ethanol and butanol ("Energy Explained," 2015).

	Units	Gasoline	Pure Ethanol	Pure Butanol
Oxygen Content	100%	Close to 0	36	22
Octane Number	100%	85 to 94	112.5 to 114	87
Reid Vapor Pressure	Bar	0.480 to 1.034	0.159	0.023
Higher Heating Value	MJ/liter	34.8	23.6	-
Lower Heating Value	MJ/liter	31.2 to 32.4	21.1 to 21.3	27.8

Table modified from "Energy Explained," 2015.

Figure 2.2: Gasoline, ethanol and n-butanol fuel properties

Among the fuel properties listed in the table above, two properties of ethanol are superior to both gasoline and butanol. Oxygen content is the first property listed in Figure 2.2. It is believed that a greater amount of oxygen in fuel allows for more complete

combustion and reduces carbon monoxide emissions ("Energy Explained," 2015). Pure gasoline has an oxygen content of around zero, compared to the oxygen content of ethanol at 36% and butanol around 22%. The second fuel property, octane rating, is the measure of temperature and pressure needed to ignite a fuel/air mixture ("Energy Explained," 2015). High octane fuels prevent premature ignition which can damage the engine. Ethanol has the highest octane rating of 112.5 to 114 while gasoline and butanol have comparable ratings of 85 to 94 and 87 respectively. In addition to ethanol's two superior properties listed above, ethanol is less toxic to humans and other species than butanol ("Energy Explained," 2015).

Although there are some advantages to using ethanol as a fuel, there are also advantages to using butanol. Reid Vapor Pressure is the minimum vapor pressure to start a cold engine. Butanol has the lowest Reid Vapor Pressure when compared to gasoline and ethanol, which means it is the most difficult type of fuel to start a cold engine with. However, the lower vapor pressure of butanol reduces the amount of harmful pollutants, such as volatile organic compounds (VOCs), released by the fuel. Scientists use two measures of heating value to measure the amount of heat energy a fuel released when a fuel is combusted; higher heating value (HHV) and lower heating value (LHV). LHV is more commonly used by scientists because it excludes the amount of heat value released to vaporize water, which cannot be utilized by common engines ("Energy Explained," 2015). As noted in Figure 2.2, gasoline has the highest LHV followed by butanol which has 86% of the LHV of gasoline and ethanol with only 65%. Butanol's superior LHV would cause the monetary value of butanol to be higher than that of ethanol.

In todays market, fossil fuels dominate the transportation fuel industry ("How we use energy ", 2015). Therefore, switching from petroleum and gasoline to biofuels will not occur overnight. Because of this, mixing biofuels with traditional liquid fossil fuels has been a common practice (Earley & McKeown, 2009). Currently ethanol is the most common biofuel additive to gasoline (Earley & McKeown, 2009). However, butanol-gasoline mixtures have a few advantages when compared to ethanol-gasoline mixtures. First, a standard vehicle engine, with no modifications, can combust any percent mixture of butanol-gasoline ("Energy Explained," 2015). On the other hand, ethanol-gasoline mixtures can only be used in standard vehicle engines when the ethanol percent is 15% or lower

("Energy Explained," 2015). Butanol mixes better with gasoline because a butanol molecule has a larger chain and therefore more closely resembles gasoline than ethanol ("Energy Explained," 2015). To add to this, butanol-gasoline mixtures do not separate in the presence of water, while ethanol-gasoline mixtures do ("Energy Explained," 2015). This factor causes extra complications in the production of ethanol-gasoline fuels because the substances cannot be mixed in storage before transportation ("Energy Explained," 2015). Also the transportation of ethanol through pipelines is not an option due to potential water contamination ("Energy Explained," 2015). Lastly, butanol's immiscibility in water would result in less soil contamination when spilled compared to a similar spill of ethanol ("Energy Explained," 2015).

Both ethanol and butanol can be produced through fermentation of sugars derived from the same type of crops ("Energy Explained," 2015) . However, using one metric tonne of sugar results in a yield of 648.2 liters of ethanol versus only 508.1 liters of butanol ("Energy Explained," 2015). The fermentation of ethanol has only one chemical reaction, producing only ethanol and carbon dioxide (Reaction 1) ("Energy Explained," 2015). On the other hand, the fermentation of butanol occurs through the acetone-butanol-ethanol (ABE) process (Reaction 2) ("Energy Explained," 2015). The ABE fermentation process produces byproducts such as carbon dioxide, water, acetone, ethanol, acetic acid, butyric acid, and hydrogen gas ("Energy Explained," 2015). The byproducts of ABE fermentation contribute to butanol's lower yield compared to ethanol.

$$C_6H_{12}O_6 \rightarrow 2C_2H_5OH + 2CO_2 \qquad \textit{Reaction 1}$$

$$C_6H_{12}O_6 \rightarrow C_4H_9OH + 2CO_2 + H_2O \qquad \textit{Reaction 2}$$

There are many advantages to using butanol as a fuel source when you compare its fuel properties to gasoline and ethanol. However, the fermentation of butanol faces a few challenges as a result of its low yield and creation of multiple byproducts. Although bio-butanol can be produced through fermentation of corn, sugar beets, etc., it is still more expensive compared to producing petroleum ("Carbon cycle 2.0," ND) In addition, due to ethanol's higher yield per bushel of corn, butanol has a higher cost ("Carbon cycle 2.0," ND). Bio-butanol is a promising biofuel for the future, however like other biofuels, more technological advances are needed in the coming years to insure its feasibility as an energy source (Earley & McKeown, 2009).

2.1.6 Bio-butanol Companies in Industry

Recently a few companies such as Butamax and Gevo have noticed the potential of bio-butanol as a biofuel source. In order to grow the bio-butanol market, Butamax and Gevo have developed new technology to produce bio-butanol. The companies discovered it is possible to cost effectively retrofit ethanol production facilities into butanol production facilities. Butamax and Gevo both make a few changes to the production plant during the retrofitting process. A few of the changes include the addition of a corn oil removal system and modification of existing equipment ("Butamax," 2016). In addition to retrofitting production facilities Butamax, also insures their clients that they will provide a secure, high-value market for all bio-butanol production ("Butamax," 2016).

The companies are both relatively new however their progress in recent years shows promise. In 2013 Butamax started its first bio-butanol retrofitting project in Lamberton, Minnesota. Today the facility is open and in full operation ("Butamax," 2016). Gevo also has a plant in Luverne, Minnesota that produces isobutanol, ethanol and related products from renewable feedstocks ("Gevo," 2016). In 2015, Butamax and Gevo decided to enter into Global Patent Cross-License and Settlement Agreements to Accelerate Development of Markets for Bio-based Isobutanol and End All Litigation ("Butamax," 2016). Previously the two companies were in competition and devoting a portion of their time and energy to litigation over bio-butanol technologies instead of their company's growth. With the new agreement, both Butamax and Gevo can focus on growing the bio-butanol industry by continuing to improve their technologies and expand the bio-butanol market.

2.2 Supercritical Fluid Extraction

Supercritical fluid extraction (SFE) is a separation process using a solvent that is above its critical pressure and temperature (Seader & Henley, 1998). First observations about using a supercritical fluid as a solvent medium were recorded in the late nineteenth century (McHugh et al., 1994). However, it was not until the 1960s that some applications of SFE were being evaluated for certain commercial processes (Seader & Henley, 1998). By the mid-1980s some SFE plants had appeared in Germany, the UK, France, and the United States for decaffeinating coffee beans, extracting hops and separating spices (Seader &

Henley, 1998). Now SFE is one of the most popular separation methods used on an analytical and preparative scale (Herrero, Mendiola, Cifuentes, & Ibáñez, 2010). The development and advancement of process equipment to support supercritical conditions and recent research on "the assessment of the industrial economical feasibility" on some developed processes shows growing interest in SFE use in industry (Herrero et al., 2010).

2.2.1 Advantages and Disadvantages of SFE

There are distinct advantages to SFE over other forms of separation such as distillation, gas stripping, adsorption, or evaporation. A wide variety of components can be recovered, at high yields, from a mixture when using a supercritical solvent that the desired substance is soluble in (Rahimi, Prado, Zahedi, & Meireles, 2011). Another advantage to using SFE is how easy it is to separate the product from the solvent by deviating from the critical pressure and temperature (Özkal, Salgın, & Yener, 2005). However, there are disadvantages to SFE. While SFE equipment is advancing and becoming more available, it requires a high investment to upscale a SFE process to manufacturing scale (Rahimi et al., 2011). There is also no recognized model or standard method to evaluate the cost of making a SFE process on an industrial scale (Rosa & Meireles, 2005). Beyond economic barriers, it is challenging to scale up a SFE lab processes because it is necessary to predict, usually via a model, the mass transfer and solubility behavior of the system on a large scale (Özkal et al., 2005). For these reasons, SFE has become a popular technique for small-scale experimentation and is not as common in industry.

2.2.2 Supercritical Carbon Dioxide as an Extraction Solvent

Supercritical carbon dioxide ($scCO_2$) is the most commonly used supercritical fluid in SFE processes (Herrero et al., 2010). There are many advantages to selecting $scCO_2$ as the extracting solvent, the main benefits revolving around safety. $scCO_2$ is non-toxic to humans and non-explosive (Özkal et al., 2005). In addition, $scCO_2$ has been considered more environmentally friendly compared to other typical organic solvents (Herrero et al., 2010). Economically, $scCO_2$ is cost effective and is one of the cheapest supercritical fluids to purchase (Özkal et al., 2005). Lastly, its chemical properties cause $scCO_2$ to have high solvent strength for non-polar compounds (Herrero et al., 2010). However, due to low

polarity $scCO_2$ is not an effective solvent choice for extracting more polar substances, limiting its potential use in some SFE applications (Herrero et al., 2010).

2.2.3 SFE of Butanol using $scCO_2$

Carbon dioxide is a predicted favorable solvent for SFE of higher molecular weight alcohols, such as butanol, from aqueous solution (Laitinen & Kaunisto, 1999b). Since butanol is less hydrophilic and volatile than lower molecular weight alcohols like methanol and ethanol, it will have a more favorable distribution coefficient (Laitinen & Kaunisto, 1999b). The distribution coefficient describes the equilibrium dispersion of butanol between water and carbon dioxide under extraction conditions (Laitinen & Kaunisto, 1999b). A previous experimental study was completed to extract 1-butanol from an aqueous solution using $scCO_2$ in a continuous countercurrent SFE column (Laitinen & Kaunisto, 1999b). This experiment found that over 99.7% of the initial amount of butanol was extracted and therefore these workers determined that it was feasible to extract 1-butanol from an aqueous solution using $scCO_2$ (Laitinen & Kaunisto, 1999b).

2.2.4 SFE of Butanol from Fermentation Broths

There are several examples in literature of $scCO_2$ being used to extract alcohol from fermentation broths in the field of biofuel research. An experiment using $scCO_2$ in lab-scale HFM contactors to extract butanol from a butanol, ethanol, acetone fermentation broth was published (Moreno, Tallon, & Catchpole, 2014). Two key parameters found and tested to improve separation efficiency in the experiment were the flow rate of the aqueous phase and the operating pressure conditions (Moreno et al., 2014). Another experiment used SFE with $scCO_2$ and solvent extraction for butanol recovery from fermentation broth (Delgado & Pessoa, 2014). $scCO_2$ was used to extract 1,3-propanediol and glycerol then solvent extraction with n-butyl-butyrate to recover butanol (Delgado & Pessoa, 2014). One of the main challenges faced when trying to extract butanol from fermentation broths is the side reaction that typically creates acetone and ethanol (in ABE process); there are metabolic engineering approaches being studied to minimize the formation of these byproducts (Oudshoorn, Van Der Wielen, & Straathof, 2009). Therefore SFE and other methods of extraction, like gas stripping and absorption, are also being tested for their feasibility and economics of being used on an industrial scale (Oudshoorn et al., 2009).

2.3 Phase Equilibrium Modeling

2.3.1 Bulk Mass Transportation

Creating models that can predict experimental data is important to analyze systems that are difficult to run experimentally. Once an accurate model has been achieved, it can be used to check the accuracy of experiments, resulting in the need for fewer experiments. By using bulk transportation of carbon dioxide and water the mass transfer coefficient ($K_l a$) of the reactor system can be determined (Wade & Simek, 2011). The simple two-film theory can be used to help understand the transfer coefficients seen in Figure 2.3 (Wade & Simek, 2011).

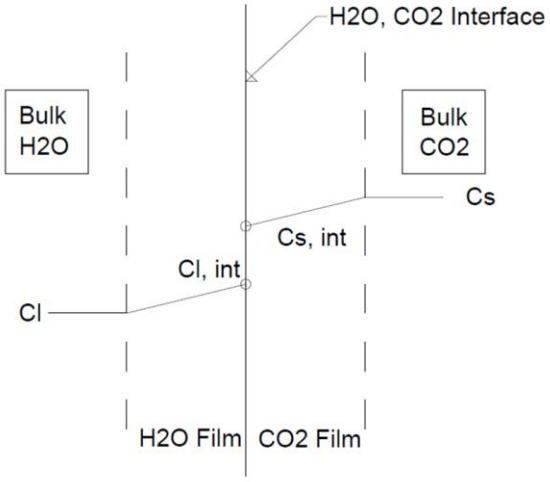

Figure 2.3: Two film theory diagram (Modified from Wade & Simek, 2011)

Applying the two film theory to the reactor system, the mass balance of butanol in the $scCO_2$ phase (Equation 2.1) and in the water phase (Equation 2.2) are shown.

(2.1) $$V_s \frac{dC_s}{dt} = -GC_S + V_1 K_l a(mC_l - C_s)$$

(2.2) $$\frac{dC_l}{dt} = -K_l a(mC_l - C_s)$$

These two equations can be solved for using Laplace transform (where s is the Laplacian variable) and the initial reactor conditions given in Equation 2.3.

(2.3) $$C_l = C_{l0} at\ t = 0$$

This gives equations 2.4 and 2.5.

(2.4) $$V_s s C_s(s) = -GC_s(s) + V_l K_l a(mC_l(s) - C_s(s))$$

(2.5) $$sC_l(s) - C_{l0} = -K_l a(mC_l(s) - C_s(s))$$

Rearranging Equation 2.4 in terms of $C_s(s)$ and plugging it into equation 2.5 gives,

(2.6) $$C_l(s) = \frac{(s+A)C_{l0}}{s^2+q_1 s+q_2}$$

Where,

(2.7) $$A = \frac{G}{V_s} + \frac{V_l}{V_s} * K_l a$$

(2.8) $$q_1 = K_l a * m + \frac{G}{V_s} + \frac{V_l}{V_s} * K_l a$$

(2.9) $$q_2 = K_l a * m * \frac{G}{V_s}$$

Rearranging equation 2.6 gives the final concentration of butanol inside the reactor at any time (t)

(2.10) $$C_l = C_{l,0} * (\beta_1 * e^{\propto_1 * t} + \beta_2 * e^{\propto_2 * t})$$

Where,

(2.11) $$\alpha_1 = \frac{-q_1 + \sqrt{q_1^2 - 4*q_2}}{2}$$

(2.12) $$\alpha_2 = \frac{-q_1 - \sqrt{q_1^2 - 4*q_2}}{2}$$

(2.13) $$\beta_1 = \frac{\propto_1 + A}{\alpha_1 - \alpha_2}$$

(2.14) $$\beta_2 = \frac{\propto_2 + A}{\alpha_2 - \alpha_1}$$

By rearranging equation 2.13, the mass transfer coefficient ($K_l a$) can be calculated using

(2.15) $$K_l a = -\frac{\propto_1 * \left(1 + \propto_1 * \frac{V_S}{G}\right)}{m * \left(\left(\propto_1 * \frac{V_S}{G}\right) + 1\right) + \propto_1 * \frac{V_l}{G}}$$

Where,

α_1 is the slope of the Ln (C_a/C_o) and is determined from experimental data
m is the partition coefficient and is 2.2 (Laitinen & Kaunisto, 1999b)
V_S is the volume of $scCO_2$ in the reaction
G is the $scCO_2$ flow rate
V_l is the volume of butanol/water mixture in the reaction
$K_l a$ is the mass transfer coefficient
C_l is the final concentration in the reactor
Cl,0 is the initial concentration in the reactor

By using equations 2.1-2.15 and collected experimental data, the final concentration of butanol in the reactor can be calculated at any time. The effects on $K_l a$ from changing pressure, initial concentration and flow rate can be determined. Once a model has been

created for a system, it can be used to scale-up the procedure or run it with other variables (Tai & Wu, 2005).

2.3.2 Transportation Through a Cell Membrane

The amount of butanol that an organism produces and releases, from its cell membrane, needs to be estimated to determine the concentration of butanol in the reactor. Because we did not run the reactor with the organism present, a model of the mass transfer through a cell membrane was created. It is assumed that the surrounding layer (water) is stagnant fluid as well as a perfect sphere, shown in Figure 2.4 (Clark & Blanch, 1997).

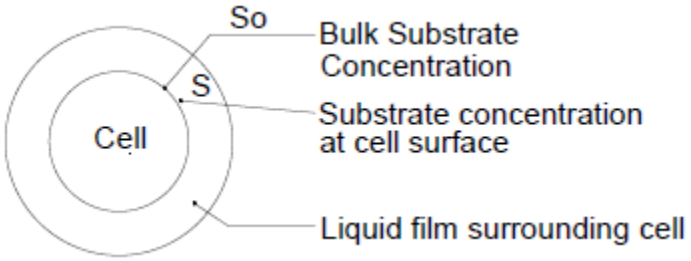

Figure 2.4: Mass transfer across a cell membrane (Modified from Clark & Blanch)

$$(2.8) \qquad Mass\ Transfer\ rate = K_L a * \left(\frac{X}{\rho_{cell}}\right) * (S_o - S)$$

Using equation 2.8, the transfer rate of butanol can be calculated with the given transfer coefficient, K_L, surface area to volume ratio of the cell, a, and the ratio of the cells volume to the solution (Peet et al., 2015). The initial bulk concentration can be assumed to be one hundred percent butanol, with the substrate concentration unknown (Clark & Blanch, 1997).

2.3.3 Butanol Phase Equilibrium

The processes of extracting alcohols or aldehydes, from water, using supercritical carbon dioxide relies heavily on the phase equilibrium of the ternary system. Experiments have been performed to determine phase equilibrium between ternary systems, in particular, n-butanol, water and carbon dioxide (Panagiotopoulos & Reid, 1986). A range of pressures were examined, from 2-15MPa, with temperatures of either 313 or 333K (Panagiotopoulos & Reid, 1986). Results were modeled using a density dependent mixing rule with a cubic equation of state (Panagiotopoulos & Reid, 1986). At the lower pressure (2MPa), the solubility of the three binary systems within the ternary system (water and n-

butanol, water and carbon dioxide, n-butanol and carbon dioxide) is low. As pressure increases, carbon dioxide and n-butanol become more soluble, while water and carbon dioxide or n-butanol do not change. Once pressure is increased to 10MPa (critical pressure of carbon dioxide), n-butanol becomes very soluble with supercritical carbon dioxide, which is shown in a complete change of the phase diagram (Panagiotopoulos & Reid, 1986).

Models showed similar trends for the different temperatures, except the effects of pressure are increased at 333K (Panagiotopoulos & Reid, 1986). Changes in temperature 333K, 343K and 353K, with two different pressures (60 and 80 bar or 780 and 1160 PSI) have been examined for the ternary system of n-butanol, water and carbon dioxide (Chen, Chang, & Chen, 2002). When pressure varied, with constant temperature, it was found, similarly to the 1986 paper (Panagiotopoulos & Reid, 1986), the solubility between carbon dioxide and n-butanol increased. However, when increasing temperature with constant pressure, it was found that the solubility of carbon dioxide and n-butanol decreased (Chen et al., 2002). Also, the solubility of water and n-butanol increased (Chen et al., 2002). In addition, the solubility of water and n-butanol increased, resulting in high temperature being unfavorable for supercritical carbon dioxide extraction.

2.3.4 Ideal Conditions for Extraction

From literature, the ideal conditions for extracting butanol using supercritical carbon dioxide can be determined. The pressure should be set to 1500 PSI (or ~100 bar). This is the lowest pressure where the phase diagram for the ternary system of carbon dioxide, water and butanol changes dramatically, showing that carbon dioxide and butanol are much more soluble at lower pressures in the critical region (Panagiotopoulos & Reid, 1986). The reactor temperature should be set to 313K (40 Celsius). This is the lowest temperature that allows carbon dioxide to become supercritical, which is needed for butanol extraction. The lowest temperature should be used because at higher temperatures (353K), water and butanol becomes more soluble, making extraction less effective (Chen et al., 2002). Figure 2.5 depicts the phase diagram for CO2 ("The Freezing Point And The Dew Point – Part 2," 2010). The low temperature, high pressure operating conditions are not only the best extraction conditions, but also the most energy efficient, leaving no

solvent residues and limiting thermal degradation (Vázquez da Silva, Barbosa, & Ferreira, 2002).

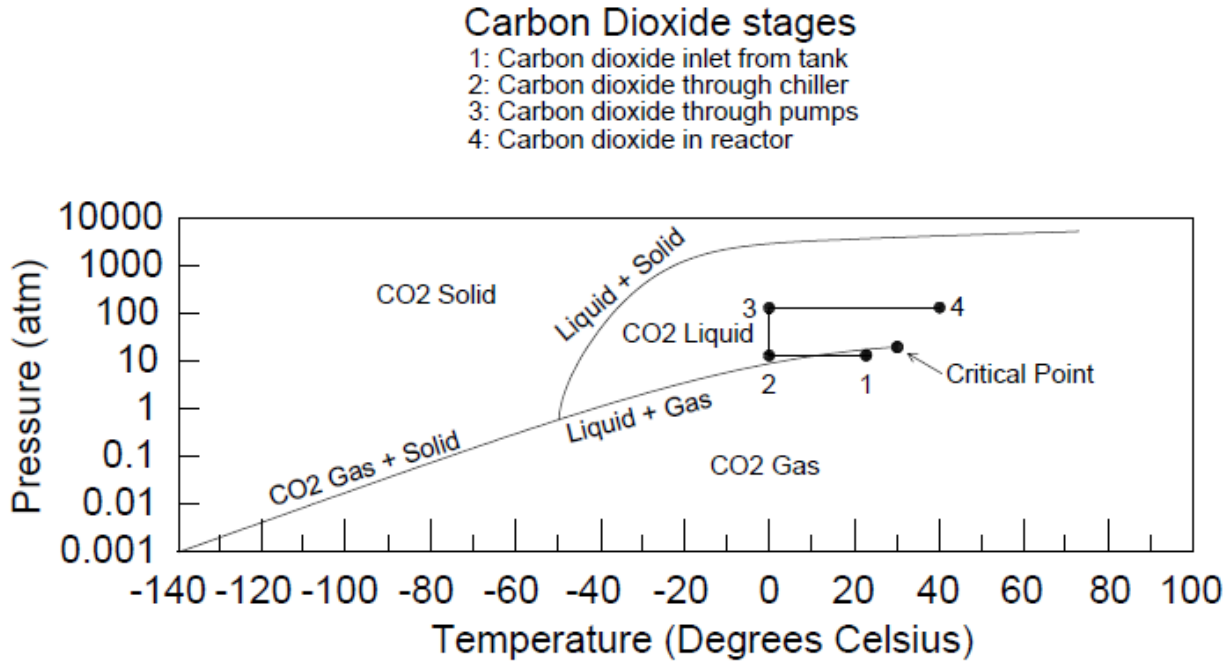

Figure 2.5: CO_2 phase diagram (Modified from The Freezing Point And The Dew Point – Part 2. (2010))

2.4 Supercritical Fluid Extraction Equipment

The basis of supercritical fluid extraction equipment starts with the reaction and separation operations. Typically a system that will create and extract butanol, or other products in a similar situation, would have two different functions consisting of reaction vessels and separation vessels. This can be carried out using a variety of different equipment including packed bed reactors, distillation columns, membrane separators, etc. One of the main reasons the processes are separated is due to the different conditions that are needed for the different unit operations. For example, an endothermic reaction might require vessels specified for high temperatures, but then to use distillation to separate the multiple products it could require a lower temperature. These separate parameters force the reaction and separation processes to be distinctly different. However, there are certain situations where reaction and separation can occur within the same range of parameters and these processes can be capitalized upon to create a more efficient system.

The butanol extraction system, in Goddard Hall, is a system that combines its reaction and separation processes. Utilizing the unique nature of an organism to produce butanol under high pressure, the system is able to use supercritical fluid extraction to simultaneously extract butanol from the reaction vessel as it is produced. Figure 2.6 shows a PFD of the system:

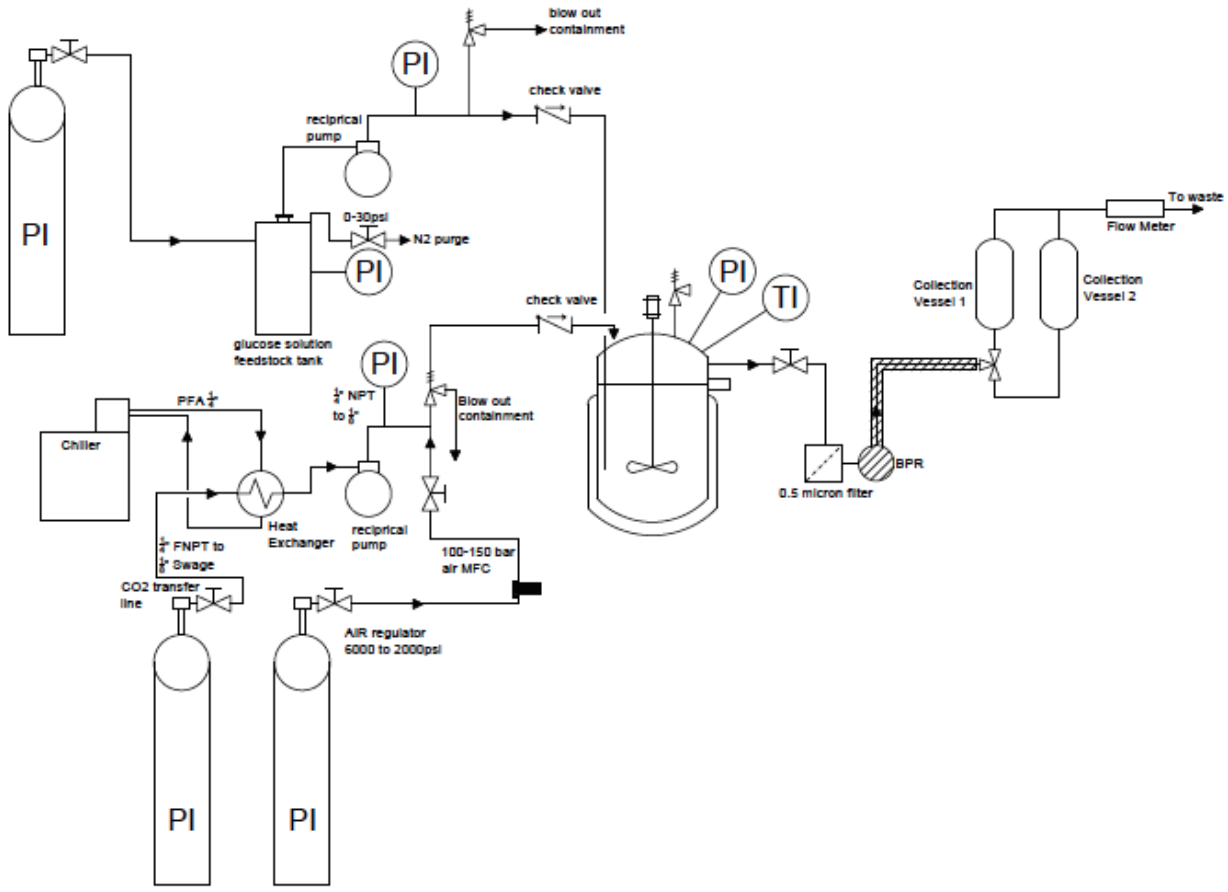

Figure 2.6: Process flow diagram of our supercritical carbon dioxide butanol extraction system

The butanol extraction system uses a carbon dioxide siphon tank to provide pressurized carbon dioxide to a Fisher Scientific Isotemp chiller (0°C). An Eldex BBB pump is used to pump the liquid carbon dioxide to the Parr reactor. The carbon dioxide fluid is then pressurized further in our system as it flows into a Parr reaction vessel coupled with a heating jacket and a reactor controller for stirring (~200-300rpm using a Rushton stirrer) and temperature control (40 °C). An Equilibar back pressure regulator (BPR) is used to maintain pressure in the reactor vessel (1500-2000 PSI), then the reactor product

depressurizes in a heated line (60C) after the BPR and flows into sample vessels that are in series and contain methanol to capture the butanol as the de-pressurized carbon dioxide gas is vented through the container. This single reaction vessel allows for a compact system that accomplishes both tasks of production and extraction and is a common technique for current work in this field.

An example of this technique can be found from Laitinen and Kaunisto, who have used a system with an Oldshue-Rushton column combined with supercritical fluid extraction. They mention in their introduction that multiple authors have tested applications for supercritical extraction in spray, sieve tray, and packed countercurrent columns. These experiments have shown great success and are very efficient and economical when compared to liquid-liquid extraction. (McHugh et al., 1994) The system that Laitinen and Kaunisto decided to test was a high-pressure bench-scale mechanically agitated Oldshue-Rushton type supercritical extraction column (Laitinen & Kaunisto, 1999a).

Laitinen and Kaunisto used a similar setup to that of the butanol extraction system, used in this work, when operating in a continuous mode. Our system has been operated in a batch mode to test the extraction time for certain weight percent samples of butanol, but in the future it will run in a semi-continuous mode to simulate the organism's constant production of butanol. The Oldshue-Rushton column used $scCO_2$ as the extracting solvent to recover ethanol from their column, while testing the effect of agitation. For their results, they were able to generate a 90 wt.% ethanol product stream from a 10 wt.% ethanol feed stream using this technique. These results show a high potential for the use of supercritical fluid extraction systems and is one of the reasons that $scCO_2$ has been chosen as our solvent for the system (Laitinen & Kaunisto, 1999a).

2.5 Extraction Safety Hazards

The safety hazards within our supercritical fluid extraction system revolve around chemical and physical risks. The chemicals used in our experiments include butanol and methanol. The physical risks center on the high-pressure system, which is necessary to create supercritical carbon dioxide.

The two chemicals in our experiment are butanol and methanol. Both pose similar health and safety risks that need to be treated with care. Both substances, when ingested, are toxic and harmful to humans so contact with skin or inhalation should also be avoided. Along with these health hazards, the substances are flammable and handled by using sparkless instrumentation and equipment. One physical risk associated with these chemicals is that during the depressurization phase, streams that are used to depressurize the system will surge periodically as the vessel loses pressure. These surges can cause sprays of butanol and this procedure should be performed carefully. To prevent these risks the operator should wear closed shoes, long pants, gloves, and safety glasses during operation (Sigma-Aldrich, 2015a, 2015b).

Supercritical carbon dioxide creates a physical threat due to its need for high pressure and low temperature. The initial advantages for using supercritical carbon dioxide for extraction in our system is that carbon dioxide is the second cheapest solvent available, after water, and it provides a chemically and environmentally safe solvent (Laitinen & Kaunisto, 1999a). Looking past these advantages, the safety aspect of this system is important to consider because it requires high pressure and subfreezing temperatures. These conditions can cause blockages and build pressure to a point where the system could fail with a blowout. The risk of substances freezing in the pipes and causing a blockage is mitigated by the use of a few mechanisms.

First, there is heating tape wrapped around the second half of our extraction system where the $scCO_2$ is depressurized, which can cause the pipes to freeze. This is usually able to prevent hazards from being created in the first place. Heating tape was also installed on the line used to depressurize the reactor to prevent ice from building up in the line and blocking the exiting carbon dioxide. Second, we have installed multiple pressure gauges in our system that are constantly monitored during the experiment to make sure that if the system does have a blockage and pressure is building then the pumps and feed of carbon dioxide can be turned off. Also there are pressure relief valves so the lines don't exceed 3000 PSI and rupture disk on the Parr reactor for pressure relief. Lastly, if the first two systems fail the extraction system is built in a carrier that has protective polycarbonate doors that are quickly and easily installed after the system is started up and under way.

These doors will be able to stop or slow down any potential projectiles or gas and liquid streams that may exit the system in an emergency.

Safety glasses and lab coats are to always be worn while running the reactor. The polycarbonate doors must be on during the operation of the system, including covering the sample jar collection area. Following an incident in the lab, the Pyrex sample jars are now stored in a metal ice bath to add an additional layer of protection. The Pyrex sample jars now installed for the system's usage also have a polymer coating to prevent from the potential glass projectiles that could be made from an over pressurized sample jar.

Chapter 3: Methodology

3.1 Reactor

Our team designed an experimental plan for the trials we conducted to test different variables: temperature, pressure, and $scCO_2$ flow rate. We created a set-up procedure to prepare the system for a run. We followed instructions and steps in order to consistently take samples from the system to analyze. Finally we documented our shutdown procedure to safely depressurize and clean the reactor.

3.1.1 Experimental Plan

Pressures

Our team varied the pressure at which the reactor functioned to see the effect of pressure on the mass transfer coefficient. The system was run as a semi-batch system, with supercritical carbon dioxide flowing into the reactor pre-charged with approximately 100 grams of a 1-wt.% solution of butanol. The system was run for 30-60 minutes at 1500 PSI, 1800 PSI, and 2000 PSI. Multiple runs at 1500 PSI were completed to validate results.

Concentrations

The effect the initial butanol concentration had on the mass transfer coefficient was studied. The initial concentration of butanol was varied while keeping the other reactor variables constant: pressure (1500 PSI), temperature (40^{o}C), agitation speed and the flow rate of supercritical CO_2. Three starting butanol concentrations were tested; 1, 2 and 3 wt.%. For each run the system was charged with 100 grams total of a water and butanol mixture, differing the proportion of butanol to water to change the weight percent. The reactor was run for 30 to 60 minutes for each trail and samples were taken in 10 to 15 minute intervals. The data was analyzed using gas chromatography. Multiple trials were performed for each weight percent to validate the data.

Mass Flow Rates

Our team analyzed their experimental data to determine the effect of changing the flow rate of supercritical carbon dioxide on the mass transfer coefficient and extraction

rate. The system was run as a semi-batch system, with the reactor pre-charged with approximately 100 grams of a 1-wt.% solution of butanol. The system was run for 30-60 minutes at 1500 PSI, with the supercritical carbon dioxide flow rate being 1.26mL/min 3.2 mL/min, and 9mL/min.

3.1.2 Set Up

Sample Jars

The samples were collected in the Pyrex sample jars (ChemGlass) containing methanol by bubbling the exit stream at atmospheric pressure. The reactor fluid was bubbled through two sample jars that were connected in series to improve the overall mass balance of the extraction. A bubble diffuser (stainless steel frit) was put at the end of the tubes to optimize the bubbling of the reactor fluid into the methanol. Before the extraction began, the sample jars were prepared by weighing the empty vials with their lids. Then methanol was added to each set of vials. 100 grams of methanol was added to the first sample jar in each series while 50 grams of methanol was added to the second jar in each series. The optimal amount of methanol to put in the sample jars was determined through a trial and error process. Too much methanol caused the gas chromatography to be less accurate, while too little methanol did not allow for the butanol to cover the diffuser in the sample jar. Every 10 to 15 minutes the sample jars were switched with two new sample jars containing fresh methanol. This allowed us to track the amount of butanol extracted at different time increments throughout the extraction.

System

The system was prepared for a run by completing a set of steps. The chiller, which was set from 0^{o}C to -6^{o}C , was turned on and allowed to cool to the set temperature. This took about 45 minutes to an hour to complete. Meanwhile, the reactor was charged with the butanol-water solution and connected to the system. Then the first two sets of sample jars were connected and placed in an ice bath. The reactor-heating jacket and the heating strips were turned on, on the lines between the back-pressure regulator and the sample jars, to reach 40^{o}C and 60^{o}C respectively. The next step was to open the valves on the pressurized carbon dioxide tank. With the carbon dioxide inlet stream being cooled by the

chiller, it entered the pump as liquid carbon dioxide. The pump was then purged before being turned on and opening the two valves on the inlet stream of the reactor. Once the pressure in the reactor broke 1000 PSI, the valve to the back-pressure regulator was opened and when the reactor reached the operating pressure, the time for the experiment was started. Sample jars were replaced consistently every 10-15 minutes.

3.1.3 Operating the system

While the system was running, one team member stayed by the system to record the time, switch out sample jars, monitor the pressure and temperature of the reactor, and make sure the pump was functioning. The sample jars were set up in series, therefore the two jars that were collecting samples had the diffusing heads, at the end of the lines, submerged in the methanol in the sample jars. However, the next sample jars that were attached to the system had the diffusers lifted out of the methanol to prevent methanol from being suctioned back and forth between the sample jars in series.

When the set time intervals were reached, the valve after the back pressure regulator was turned to the already attached next set of sample jars and the diffuser heads were submerged in the methanol. The previous sample jars were removed and capped to prevent methanol from evaporating. The next set of sample jars were then attached with the diffusers at the end of the lines out of the methanol samples that were kept on ice.

The pressure of the reactor and back-pressure regulator was monitored for consistency. The pressure gauge on the carbon dioxide inlet line was checked to verify the carbon dioxide tank was not empty. The pump had a chamber above it with an inspection port. The chamber had water in it so that it was visible if the pump was running or not. This inspection port was monitored throughout the experiment to make sure that the pump was continuously flowing supercritical carbon dioxide into the reactor. This is a high pressure sight gage used to saturate the CO2 so it does not remove too much water from the reactor

3.1.4 Shut Down

Sample Jars

After each 10 to 15 minute increment, when the sample jars were collecting the exit stream, the sample jars were removed and prepared for analysis using the gas

chromatograph. First the two sample jars in each series were weighed and the weights were recorded. Then the liquid from the two sample jars in each series were combined and mixed together. The mixture was stirred before a small sample was taken and put into a gas chromatography vial (1.5mL). Another 10 mL sample was taken and put into a separate vial for storage. The storage was used in case the data for a particular run had to be retested by the gas chromatograph. The remainder of the liquid was disposed of in the proper waste containers. This process was done for each set of vials throughout all of the reactor runs performed.

System

Following the 30 minute to an hour long trials, the system was shut down following a standard set of steps. First, the pump was switched off at the same time that the first valve on the inlet line to the reactor was closed. The second valve, right below the reactor on the inlet stream, was also closed and then opened at the end of the depressurizing process. The carbon dioxide tank was closed and the water chiller was shut off. The heating tape between the backpressure regulator and the sample jars were shut off. The heating jacket was kept on until the depressurizing process was completed.

The valve before the back-pressure regulator valve was closed and the heating tape of the metal purging line and valve was turned on to the third setting. The metal purging line was inserted into the cap of the 1000 mL Pyrex jar. The purging line from one of the sample jars was then inserted into the other opening in the cap of the 1000 mL Pyrex jar. Then the depressurizing process could begin by adjusting the valve of the metal purging line. If the line became cold or began to frost over then the valve was closed and waited to heat up. After the reactor was below 1000 PSI, the plastic purging line connected to the reactor could also be used to depressurize the system. The two lines were utilized to bring the pressure of the reactor down to atmospheric pressure.

After depressurizing, the heating jacket was removed and the second valve on the inlet stream was also closed. The reactor was then disconnected from the inlet stream and then the clamps holding the reactor in place were also removed. The remaining liquid in the reactor was added to the 1000 mL Pyrex jar where the rest of the residue was collected from depressurizing the system.

3.2 Gas Chromatography

3.2.1 Calibration

Before any samples from reactor runs were analyzed using the gas chromatograph (Shimadzu GC-MS-FID 2010) a calibration curve was created. Known weight percent mixtures of butanol and methanol were prepared and butanol in water. The weight percent of butanol ranged from 0.1 wt.% to 3 wt.%. We predicted the samples we would be analyzing would fall in this range and therefore line up with our calibration curve. After the prepared butanol and methanol samples were run through the gas chromatograph, the data was exported. From the data we plotted the calibration curve. The weight percent of butanol in each sample was put on the x-axis and the area corresponding to the peak of butanol, recorded by the gas chromatograph, was put on the y-axis. To ensure an accurate calibration curve, five calibrations were created.

3.2.2 Analyzing Samples

After the calibration curve was created, samples with an unknown weight percent of butanol were analyzed by the gas chromatograph. The area under each peak corresponding to butanol were recorded and then plotted on our calibration curve. From the calibration curve we determined the weight percent of butanol each sample contained. Therefore, the amount of butanol extracted throughout different time periods, when running the extraction unit, was known. When each set of samples were run through the gas chromatograph, a calibration vial with a known weight percent of butanol was run through as well. This allowed us to match up our calibration curve with a known weight percent of butanol and ensure that the gas chromatograph was functioning properly with each use.

3.3 Experimental Model

To model the experimental data, a kinetic based model was adapted to estimate the mass-transfer coefficient of the butanol reactor extraction (Tai & Wu, 2005). The Tai and Wu mass transfer model is similar to our butanol extraction process however their system modeled the extraction of ethanol. The Tai and Wu model is based off the two-film theory principles.

3.3.1 Model Procedure

Data collected from the extraction of butanol from water, for different weight percent, pressure and $scCO_2$ flow rate, was fitted using the Tai and Wu model for ethanol extraction (Tai & Wu, 2005). The model was adjusted to model butanol extraction by changing the equilibrium constant (m) to 2.2 for butanol (Laitinen & Kaunisto, 1999b). Adjusting the constant values of the model to match the reactor system allowed accurate modeling of the reactor. Data collected from literature shows that the concentration of butanol inside the reactor decreases over time, but the shape of the curve depends on the parameters that will be varied: Pressure, $scCO_2$ flow rate and initial concentration (Tai & Wu, 2005). Taking the natural log of the concentration of butanol left in the reactor divided by the initial concentration of butanol in the reactor, will result in a straight curve with a negative slope. The slope of this curve is known as alpha one (α_1). By plugging α_1 and the operating conditions into equation 2.15, The K_la value can be calculated. By using this K_la value, q_1 and q_2 can be found using equations 2.7-2.9 respectively. Plugging these values into equations 2.11 and 2.12, α_1 and α_2 are solved for. $\beta 1$ and β_2 are then solved for using equations 2.13 and 2.14 respectively. Finally, using equation 2.10, the concentration (C_l) at any time (t) can be calculated.

3.4 Theoretical Model

In order to validate the K_la value obtained from our experimental model, theoretical models based on extraction correlations were pursued to determine if a similar value could be calculated. Our extraction process was investigated and then assumptions were made to base correlations to begin the creation of the theoretical model. Following this, the value for K_la was calculated by separately calculating the local mass transfer coefficient (K_l) and the interfacial area (a). Overall, the calculation was based on the initial assumptions and the scenario being modeled as it could be interpreted in various ways.

When looking at the scenario for butanol extraction, the key elements considered were the extraction environment and the extraction components. The environment of the butanol extraction system could have been simply analyzed as a liquid-gas extraction system that used carbon dioxide gas to extract butanol from liquid water, but the conditions of the reactor vessel cause the carbon dioxide to behave more like a liquid at its

supercritical state due to its high increase in density (Tai & Wu, 2005). This density increase was vital in our assumption of a liquid-liquid extraction scenario for our system of water-butanol-supercritical carbon dioxide components.

After the liquid-liquid extraction assumption was made, research into correlations for similar systems was completed to finalize the equations used for which calculations. The variables, K_l and a, were calculated separately because the correlation for K_l was initially discovered in a text called *Diffusion: Mass Transfer in Fluid Systems* where Edward Cussler, the author, predicted K_l was based off of a series of different scenarios that could be applied to our system (Cussler, 2009). Multiple correlations were taken from the text and used to find the overall K_la value. All of the correlations contained an assumed interfacial area value that was calculated by adding the cross sectional area of the reactor and the surface area of the bubbles. This was considered reasonable because the interfacial area is created by the cross sectional area between the two phases and the surface area of the bubbles moving through the water phase. Then correlations for the interfacial area were investigated in literature to find an equation that would produce the assumed interfacial area used in the initial K_la calculation.

Chapter 4: Results

4.1 Gas Chromatography

A graph containing the output data of the gas chromatograph (GC) was plotted in order to validate the proper functioning of the gas chromatograph as well as the accuracy of the standard samples. In Figure 4.1 the retention time versus the signal intensity is plotted. The graph shows that as the concentration of the standard samples increased the intensity of the peaks recorded by the gas chromatograph also increased. This positive linear trend provides proof the chromatograph and the standard samples follow the expected trend.

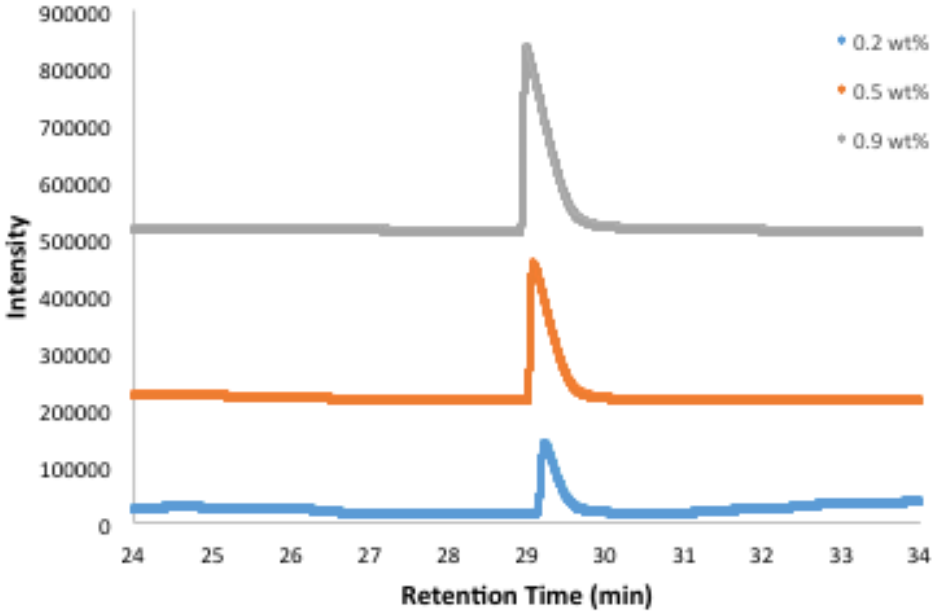

Figure 4.1: Retention time vs GC-FID intensity signal for different wt.%

4.1.1 Calibration Curves

Five separate calibration curves for butanol and methanol mixtures were developed. Of the five calibration curves developed, the curve with the highest r^2 value was used to analyze data from experimental runs. All five calibration curves can be seen in Figure 4.2. The calibration curve with the highest r^2 value (run 2) can be seen in Figure 4.3.

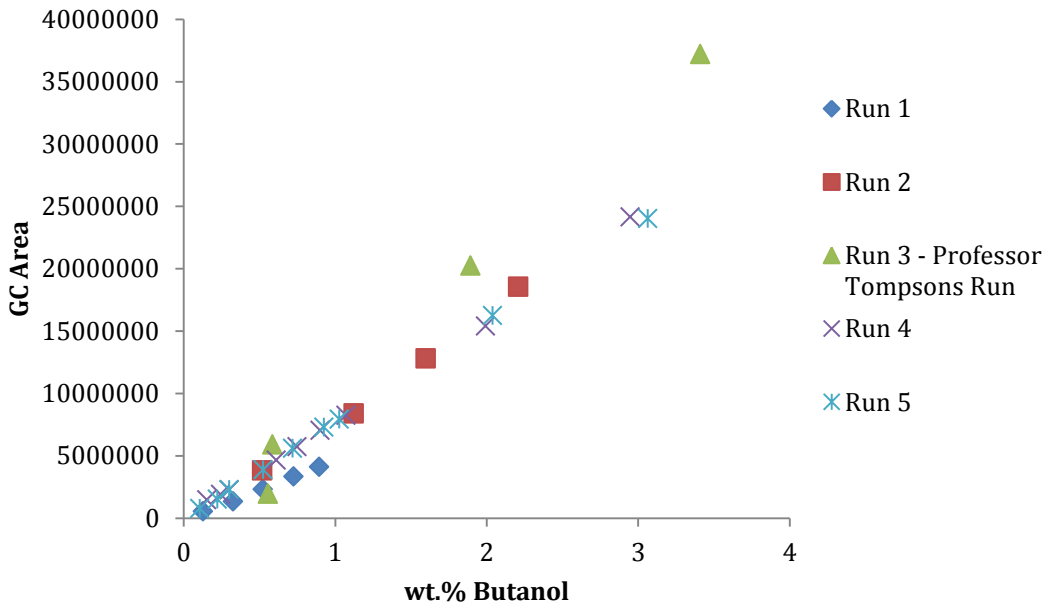

Figure 4.2: Five calibration curves for butanol and methanol standards

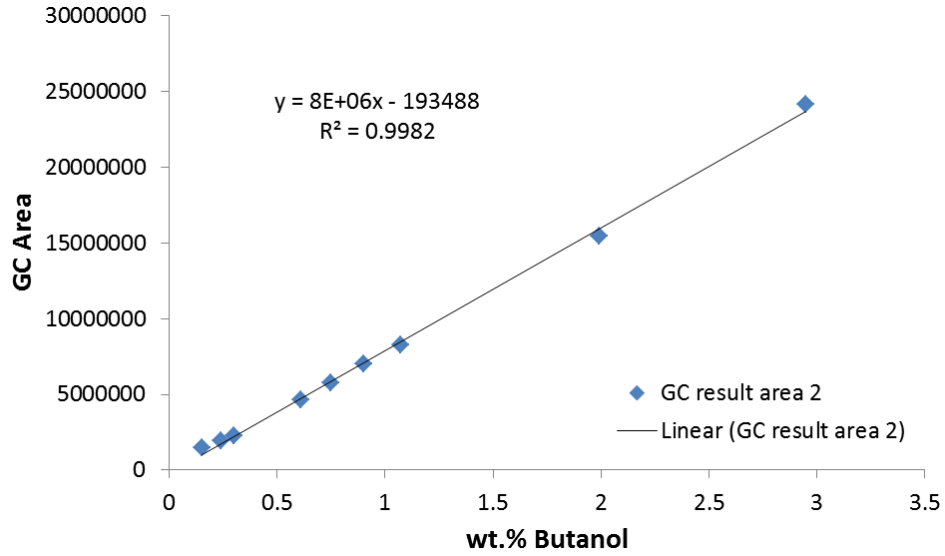

Figure 4.3: Chosen calibration curve for butanol and methanol standards (Run 2)

In addition to calibration curves for butanol in methanol, a calibration curve for butanol in water was developed. When the experimental runs were finished some butanol and water remained in the reactor system. In order to accurately predict the concentration of butanol in the water solution, we created a calibration curve which can be seen in Figure 4.4.

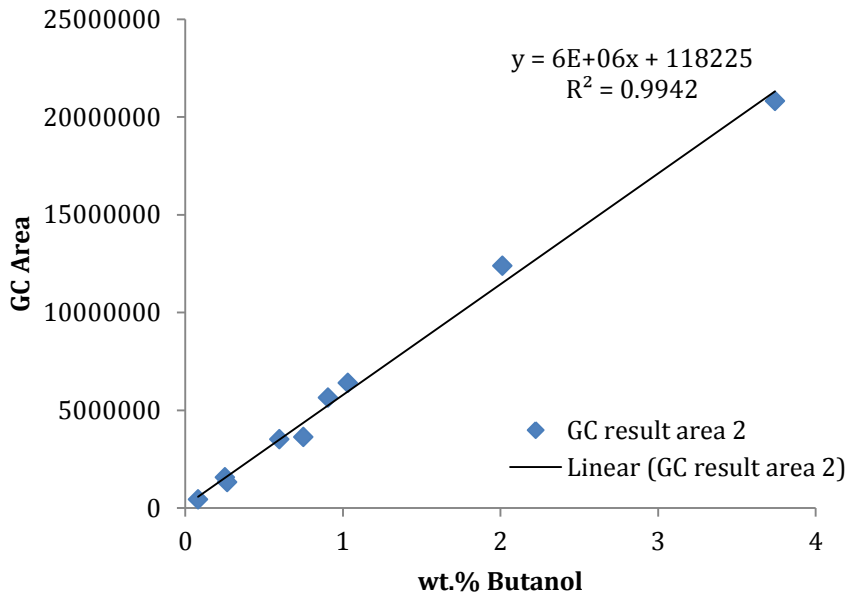

Figure 4.4: Calibration curve for butanol and water standards

The extraction samples obtained during experimental runs were measured using the gas chromatograph. A standard sample was run through the gas chromatograph with each set of unknown samples. This allowed us to ensure that the gas chromatograph was functioning properly for each run and would validate the accuracy of our calibration curve over time. There were a few cases when the standard sample did not match up with our methanol/butanol calibration curve; most likely due to variations in the functioning of the gas chromatograph. In these cases, the set of samples were run through the gas chromatograph a second time. When the samples were run a second time, the standard samples always lined up with the calibration curve. For consistency, the gas chromatograph data was used only when the standard sample agreed with our methanol/butanol calibration curve.

4.2 Experimental Results

4.2.1 Mass Balances

For each experimental run, the GC results of the samples were used to complete a mass balance around the system. With the initial amount of butanol added to the reactor recorded, the amount removed during each time interval was calculated and the residue leftover in the reactor was analyzed in the GC to determine the amount of butanol that

remained in the reactor at the end of each experiment. The desired percent error was less than 20% for each run.

After analyzing the mass balances for the first several runs, the mass balances were producing results with percent errors greater than 20%. The larger margin of error might be due to butanol escaping through the vent line. With a smaller desired percent error, the system was modified to run in series so the extraction line would bubble through a first sample jar of methanol and then a second, smaller sample jar. This would ensure that butanol in the extraction line would be bubbled through two sample jars before the carbon dioxide could be vented out of the system to exhaust. Running the system with this set up decreased the mass balance percent error to be between 5-20% depending on the run.

4.2.2 Raw Data Results on Extraction Rates for Different Parameters

After multiple procedural changes were made to how the extraction system operates a final set of butanol extraction data was obtained to show the effects of parameter changes. The three main parameters that were changed in this extraction system were initial butanol concentration in the extraction vessel, the pressure at which extraction occurred, and the mass flow rate of the $scCO_2$ flowing through the system. These parameters were chosen because they were expected to be able to shift the extraction rate of the system in a favorable direction and possibly influence how the extractor will operate in the future when *B. Megaterium* is added to the system.

Changing Initial Butanol Concentration

The initial butanol concentration in the extraction vessel was varied from 1-3 wt.% of a 100 to 150 g starting solution. This range was chosen because the organism that will be producing butanol is predicted to only reach these levels of sustainable production. Figures 4.5-4.7 show the raw data of the results for 1-3 wt.% butanol concentration.

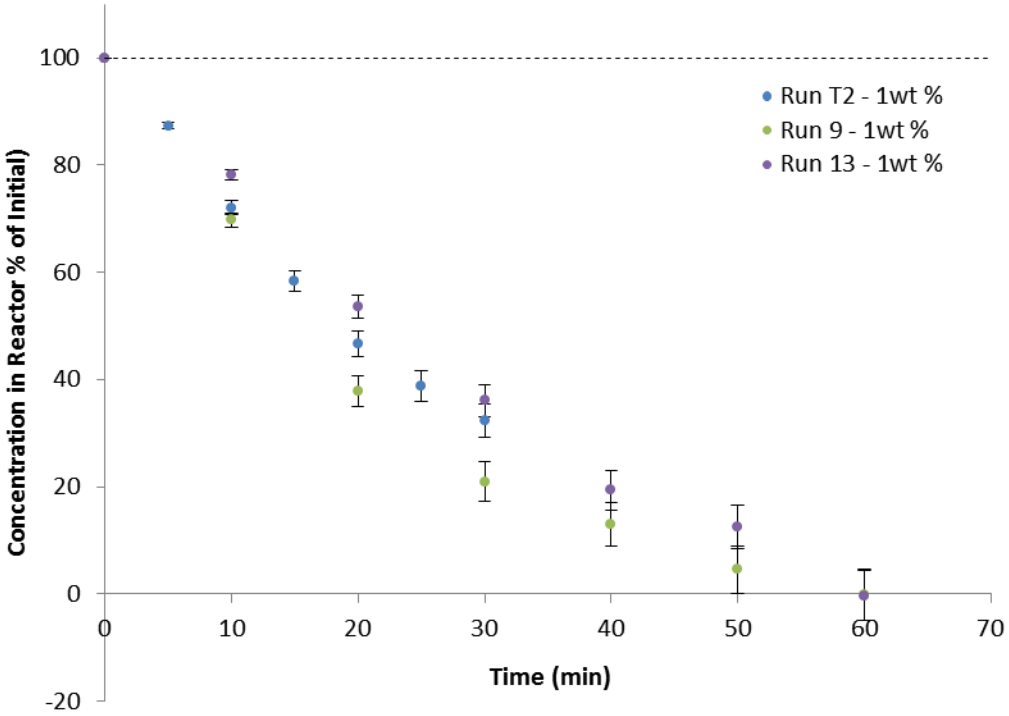

Figure 4.5: Raw data of best runs for 1 wt.% butanol

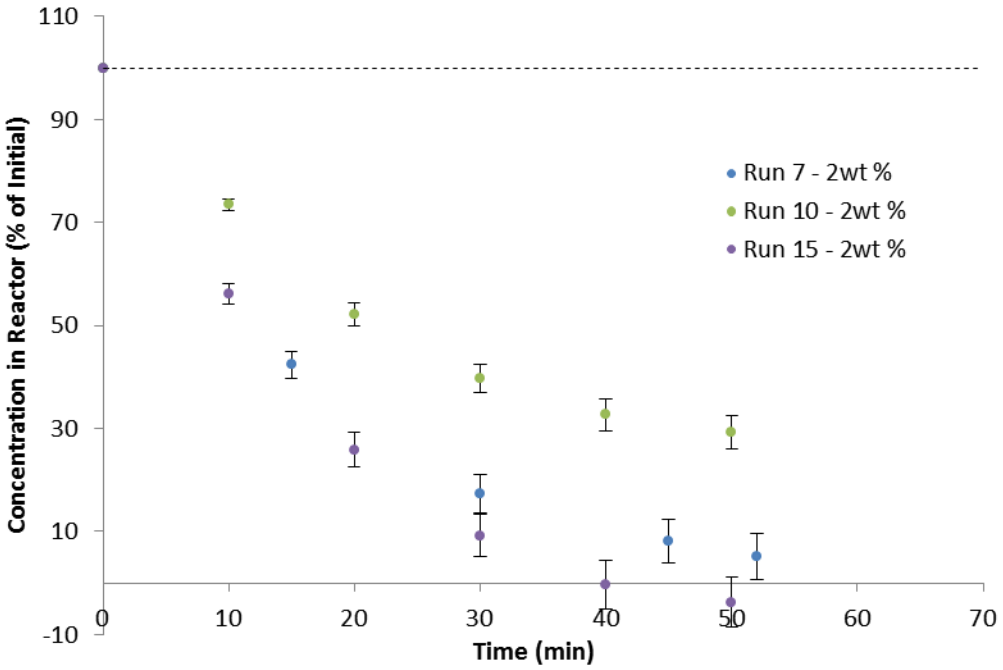

Figure 4.6: Raw data of best runs for 2 wt.% butanol

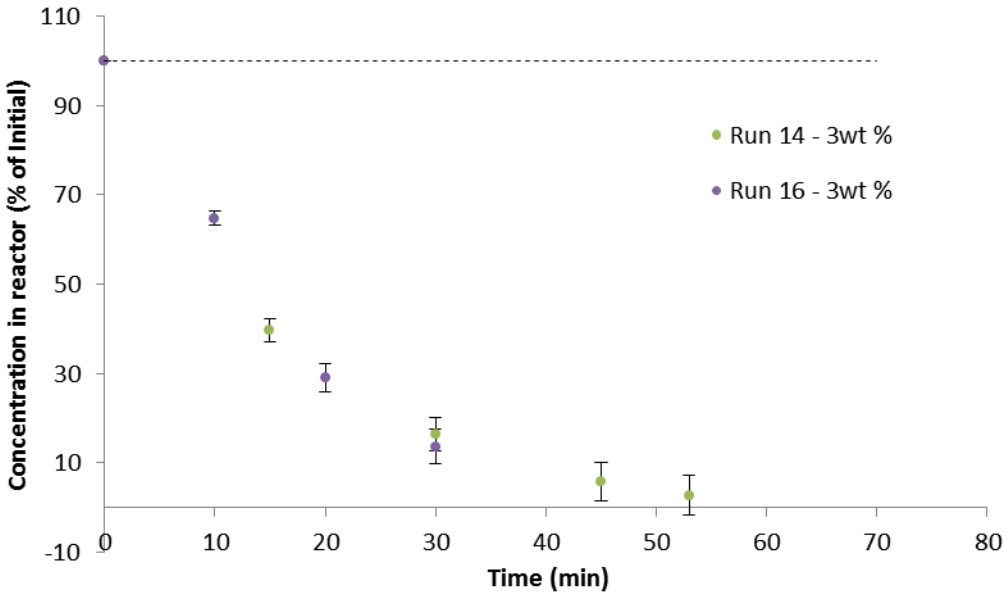

Figure 4.7: Raw data of best runs for 3 wt.% butanol

From looking at each of these graphs it is clear that the 1 wt.% and 3 wt.% data was more reproducible than the 2 wt.% data. The end result is therefore shown in terms of 1 and 3 wt.% data only as the addition of 2 wt.% does not attribute anything to the result (the 2 wt.% data overlaps almost entirely with the 3 wt.% data and is not as consistent from trial to trial). The comparison of the 1 and 3 wt.% data is shown in Figure 4.8 and predicts that there may be a trend for how concentration change affects extraction rate, which is discussed later.

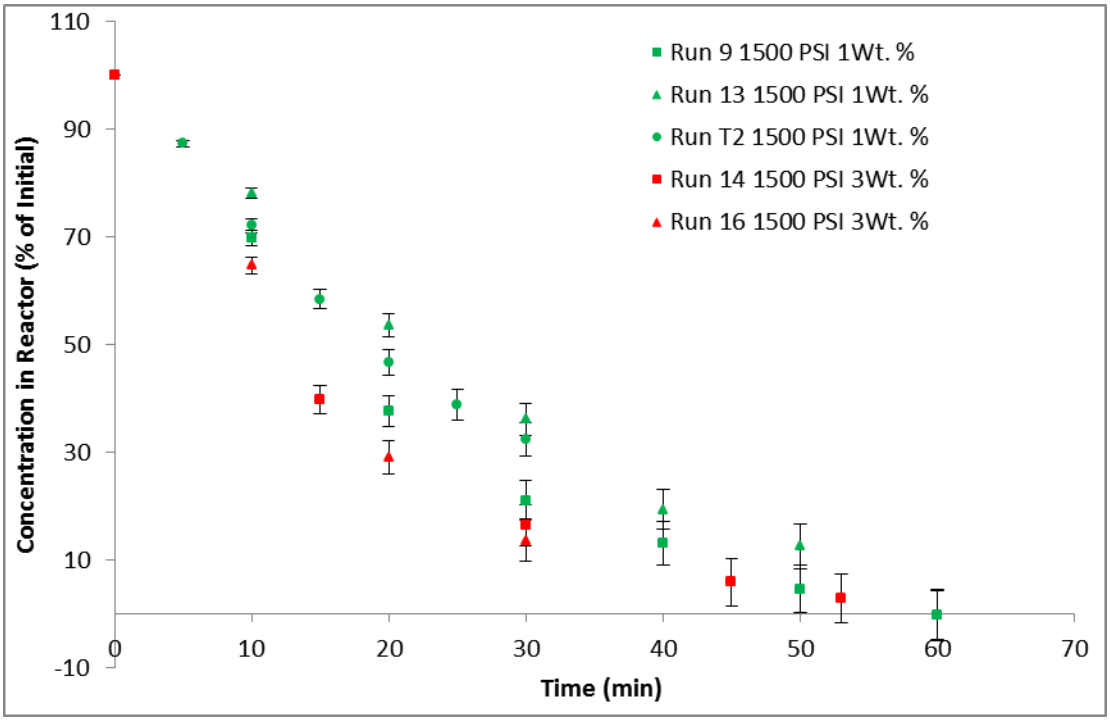

Figure 4.8: Comparison of raw data for 1 and 3 wt.% butanol concentration

Changing Operating Pressure

The pressure of the extraction system was also varied substantially to determine its impact on the extraction rate The extraction system was built for a max pressure of 3000 PSI and pressures between 1500-2500 PSI were tested for the extraction of butanol. However, after having pump problems the only run completed at 2500 PSI was not considered useable for the data collected due to large pressure variances. Figure 4.9-4.11 shows the extraction data for changing pressures at a constant 1 wt.% initial butanol concentration.

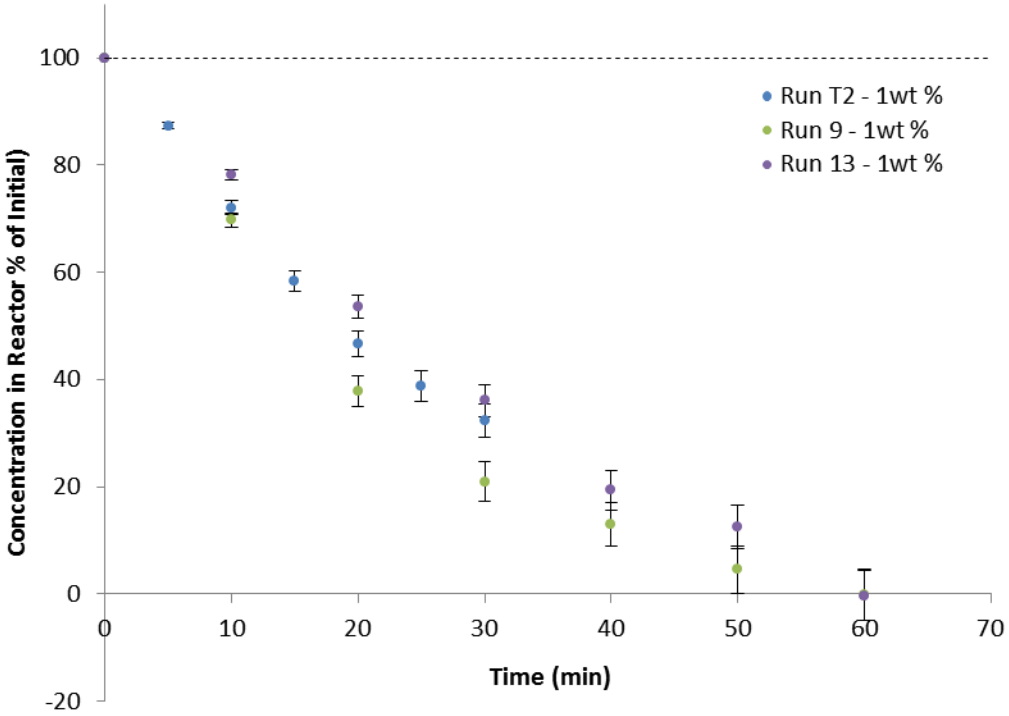

Figure 4.9: Extraction results for system operating at 1 wt.% butanol and 1500 PSI

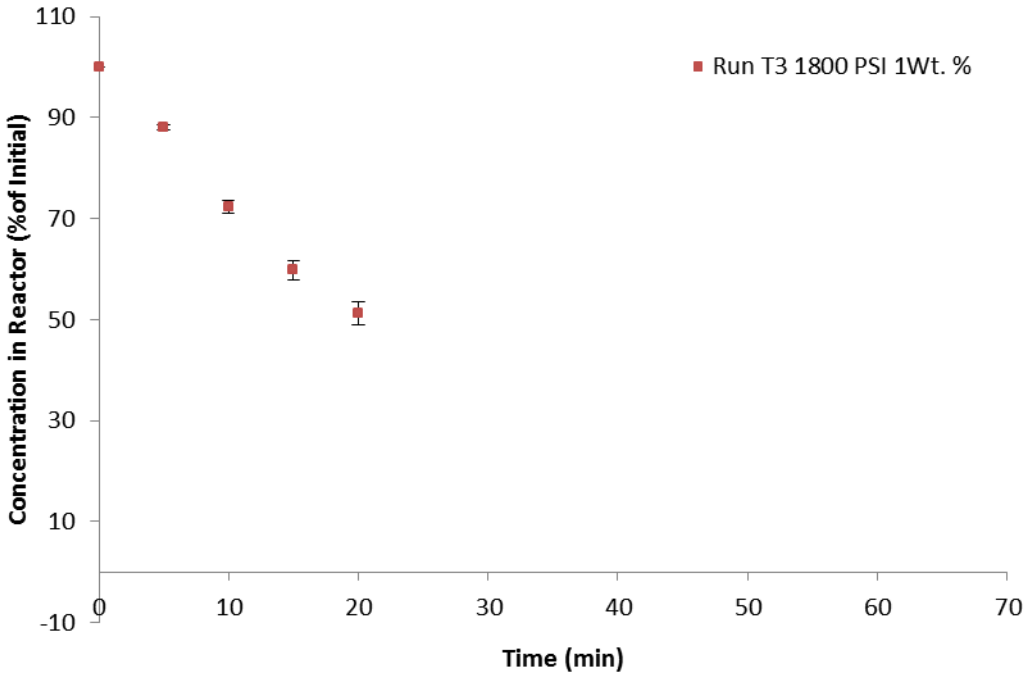

Figure 4.10: Extraction results for system operating at 1 wt.% butanol and 1800 PSI

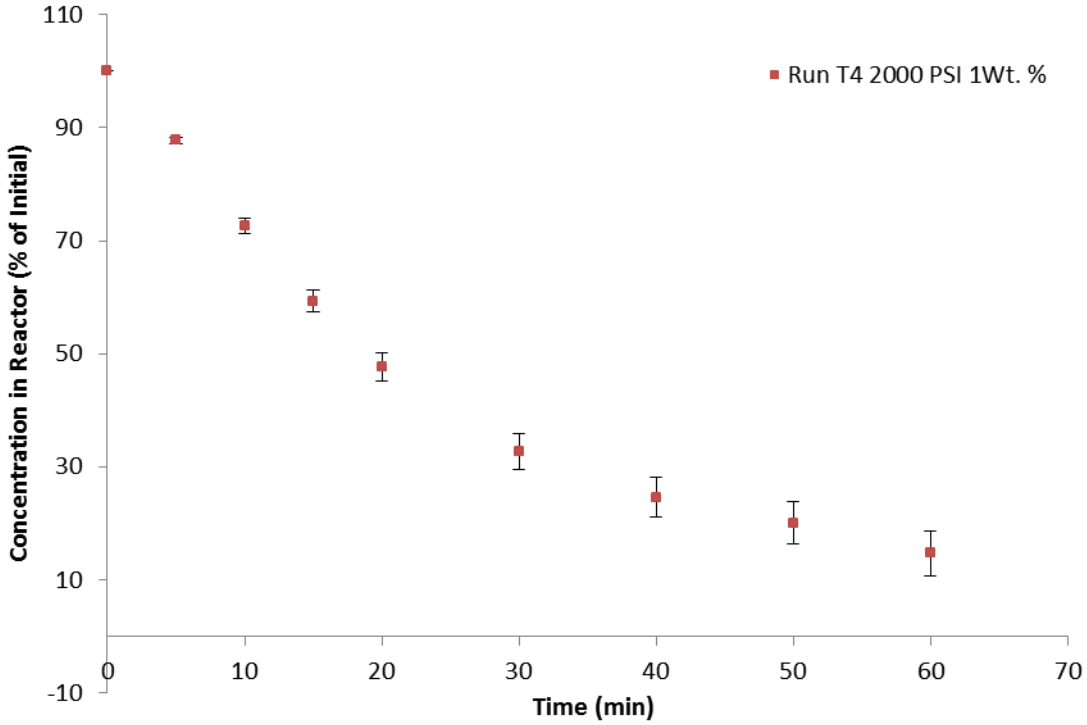

Figure 4.11: Extraction results for system operating at 1 wt.% butanol and 2000 PSI

It is clear that since 1500 PSI was the pressure used in the majority of our runs it will be the most accurate data and have the most trials, however due to system strain only one run was conducted at each elevated pressure to see if any clear trends were showing. Figure 4.12 shows all three sets of pressure data and how the resulting trend looks.

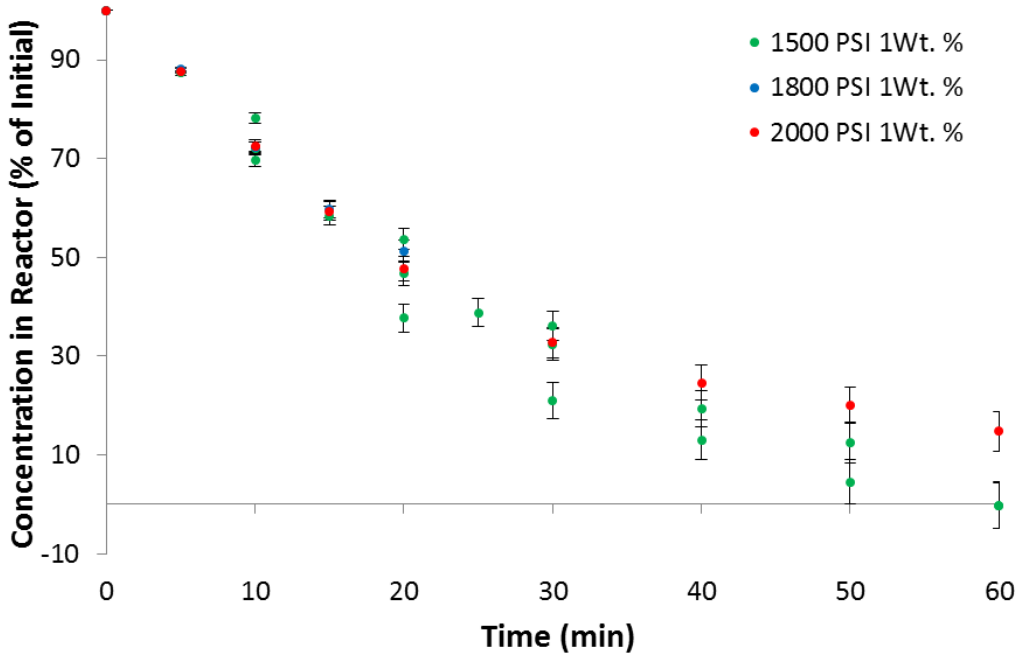

Figure 4.12: Extraction results for system operating at 1 wt.% and 1500-2000 PSI

Looking at the final graph to compare all of the pressure changes it can be seen that there is no significant change in extraction rate with a change in pressure. The overlap of the majority of the points indicates pressure change is not having an impact on the extraction rate. If there is an impact on the system due to pressure it is negated by multiple factors because the data collected does not reflect meaningful changes. Further investigation into these trends could be done to generate more reliable and repeatable data, however these initial studies show no general trend. Pressure has little affect on extraction rate.

Changing Mass Flow Rate of $scCO_2$

The final parameter of the system varied was the mass flow rate of $scCO_2$. The goal of this test was to see if changing the mass flow rate of the $scCO_2$ would affect the extraction rate of the system. These parameters were only tested in one trial each and the other variables were held constant at an initial butanol concentration of 1 wt.% and a pressure of 1500 PSI. The mass flow rate of the system was changed twice from 1.26 mL/min to 3.2 mL/min and 9.0 mL/min and this raw data can be seen in Figure 4.13.

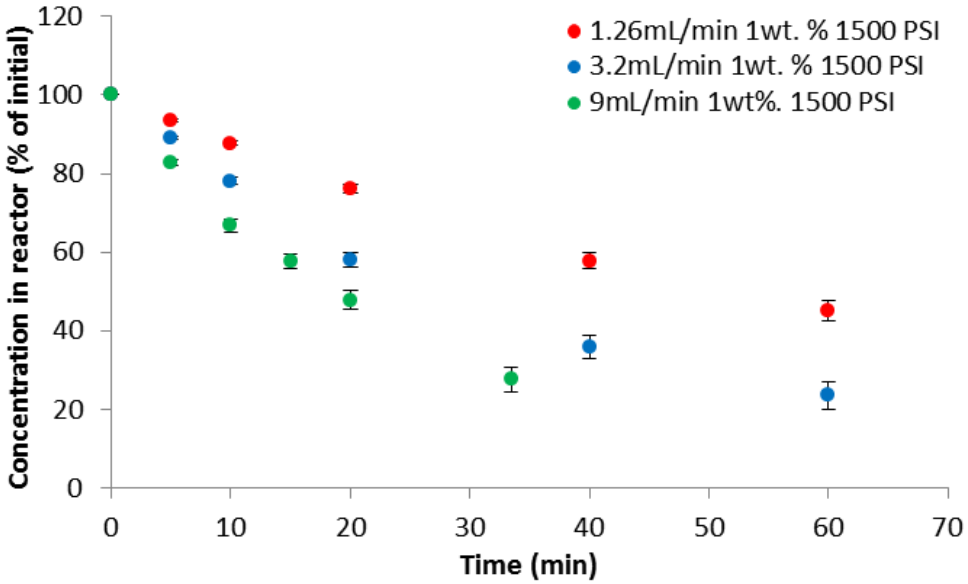

Figure 4.13: Mass flow rate of $scCO_2$ changes for system operating at 1 wt.% and 1500-2000 PSI

The trends from this graph create clear distinctions in extraction rates as the 3.2 mL/min run has a faster extraction than the 1.26 mL/min run, and the 9 mL/min run is the fastest extraction of them all. At the twenty minute mark, the three runs are as follows, the 1.26 mL/min flow has 76.0% of the butanol left in the reactor while the 3.2 mL/min run has 58.2% of the initial butanol left in the reactor and the 9 mL/min run has 47.9% of the butanol left in the reactor. This shows that the 9 mL/min run has slightly over double the extraction rate as the 1.26 mL/min run when the mass flow rate is seven times larger. With this initial data it is clear there could be an increasing trend of extraction rate with mass flow rate of the $scCO_2$ solvent. However, for this to be confirmed, a few more experiments should be run to determine if the data is reproducible and also whether this affect plateaus at some level. From a first glance, this data gives a positive look at how the mass flow rate can make this system more efficient.

4.3 Experimental Model

The extraction rate of butanol, for varying concentrations, pressures and mass flow rates can be seen from the collected data in Figures 4.8, 4.12, and 4.13. Plotting the natural log of C_a divided by C_o verse time, for varying concentration gives Figure 4.14.

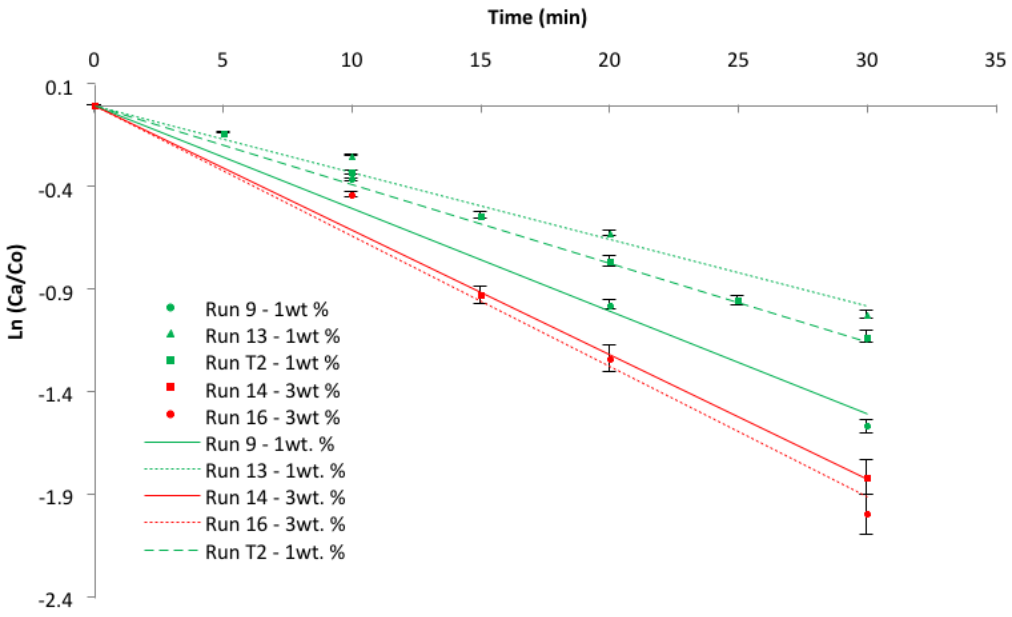

Figure 4.14: Finding the slope of $ln(C_a/C_o)$ for all 1 and 3 wt.% runs

The first alpha value, for each run, is the best fit slope value from Figure 4.14. These first alpha values from each run are shown in Table 4.1. Plugging this alpha value, as well as the constants V_s, V_l, G and m values into equation 2.15 gives the $K_l a$ value for each run. Once the $K_l a$ value is calculated, it can be plugged into equations 2.7-2.14, the concentration inside the reactor can be modeled at any time.

Run Number	Slope value (α_1)
9 – 1 wt. %	-0.000883
13 – 1 wt. %	-0.000573
T2 – 1 wt. %	-0.000648
14 – 3 wt. %	-0.001006
16 – 3 wt. %	-0.001129

Table 4.1: Slope values for all 1 and 3 wt.% runs

Figure 4.15 and Figure 4.16 show the natural log of C_a divided by C_o verse time, for runs varying pressure and flow rates respectively. These graphs show the slopes that were used for each run's first alpha value.

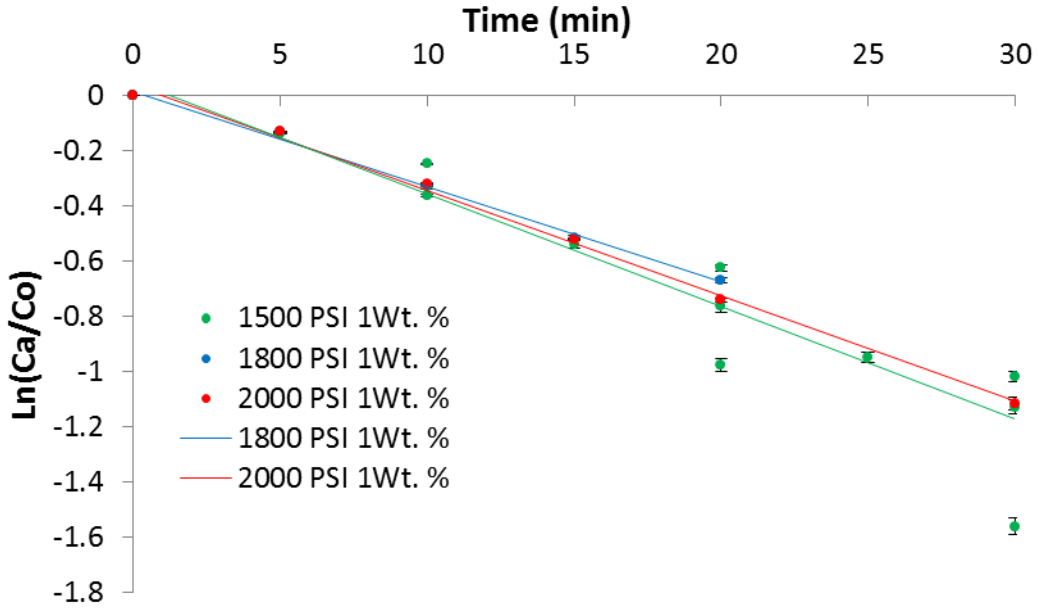

Figure 4.15: Finding the slope of $ln(C_a/C_o)$ for runs with varying pressure

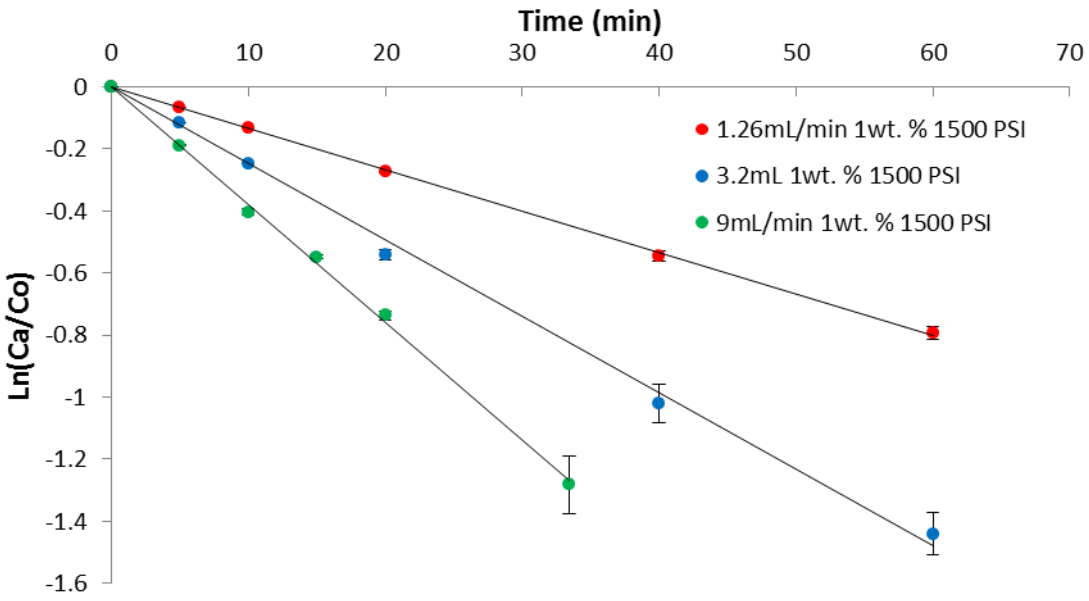

Figure 4.16: Finding the slope of $ln(C_a/C_o)$ for runs with varying flow rates

4.3.1 The Effects of Concentration on $K_l a$

To analyze the effect concentration has on the initial $K_l a$, the system was kept constant at 1500 PSI, 40°C and a $scCO_2$ flow rate of 1.26mL/min. The initial concentration tested was 1, 2 and 3 weight percent butanol in a 100 gram water mixture. Repeating the procedure above, the initial $K_l a$ was calculated and is shown in Figure 4.17 for 1 and 3 weight percent. As initial concentration increases, the initial $K_l a$ value slightly increases. Once the initial $K_l a$ value is found, the concentration inside the reactor at any time can be modeled. Figure 4.18 compares the collected data points versus the experimental model for 1 and 3 weight percent.

The increasing mass transfer coefficient with increasing concentration is physically possible because when the solution contains a higher concentration of butanol, the probability that the $scCO_2$ will collide with butanol is greater, as there are more butanol molecules.

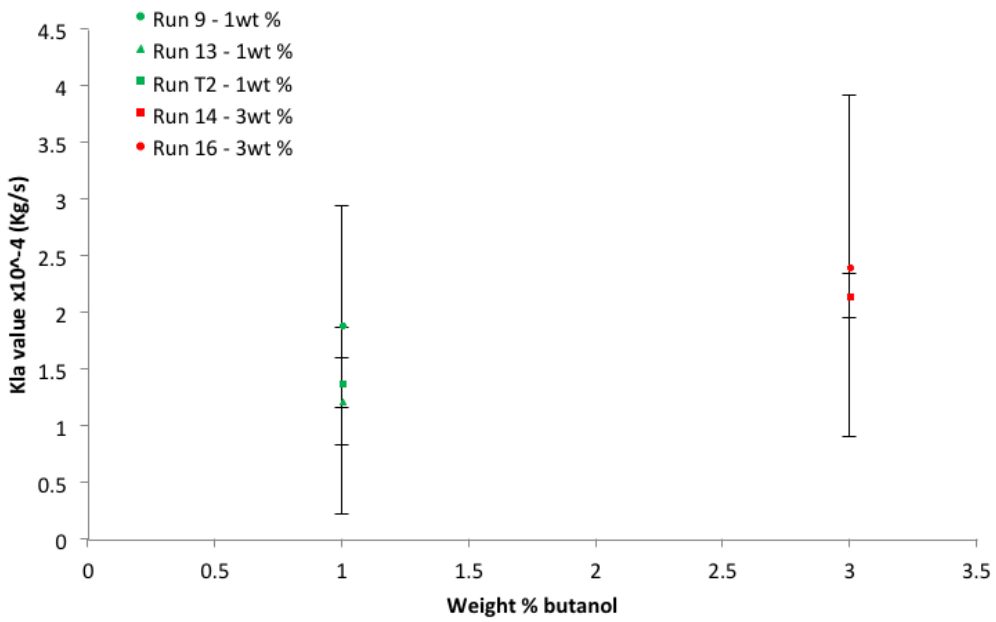

Figure 4.17: The effect of initial concentration on K_la

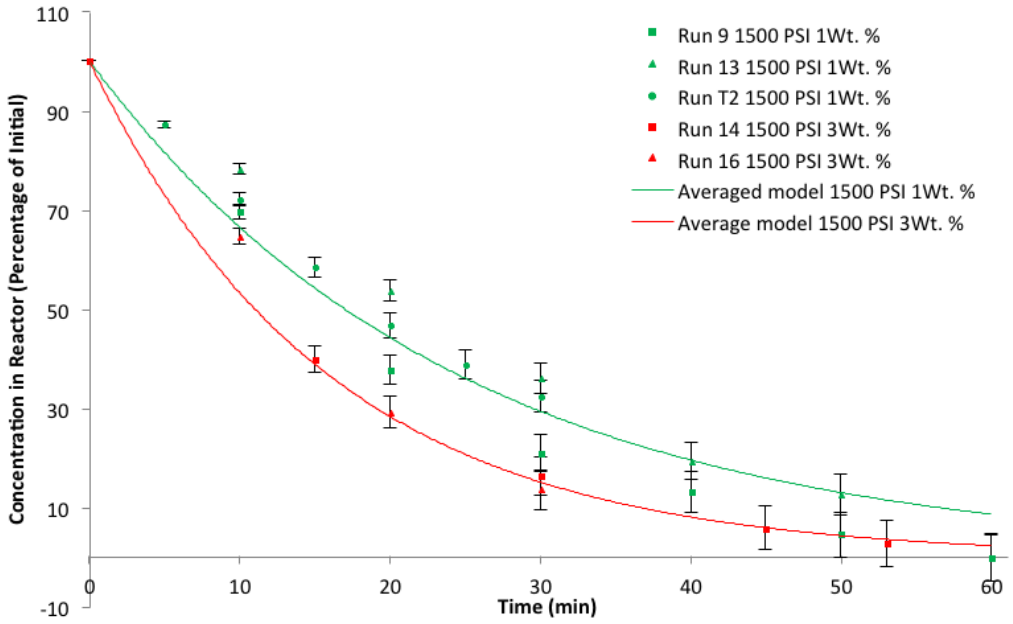

Figure 4.18: Experimental data compared to model trends for initial concentration change

Figure 4.18 indicates that generally the 3 wt.% data (red line) extracts quicker than the 1 wt.% data (green line). This trend is speculated due to the fact that the increased initial butanol concentration has a decreasing affect on the surface tension of the supercritical carbon dioxide bubbles that are entering the vessel, which would cause the

bubbles to be smaller and produce more surface area. Overall, the error in this data is reasonable, however more data would need to be collected to fully validate the trend.

4.3.2 The Effects of Pressure on $K_l a$

The pressure of the system was run at 1500, 1800 and 2000 PSI, while the rest of the system was kept constant, at 1 weight percent, 40°C and a flow rate of 1.26mL/min. Figure 4.19 shows the initial $K_l a$ value at 1500, 1800 and 2000 PSI. The figure shows that there is no distinct affect of pressure on the initial $K_l a$ value. Figure 4.20 shows the model versus the collected data points for each run, which also indicates no trend in initial $K_l a$ is found.

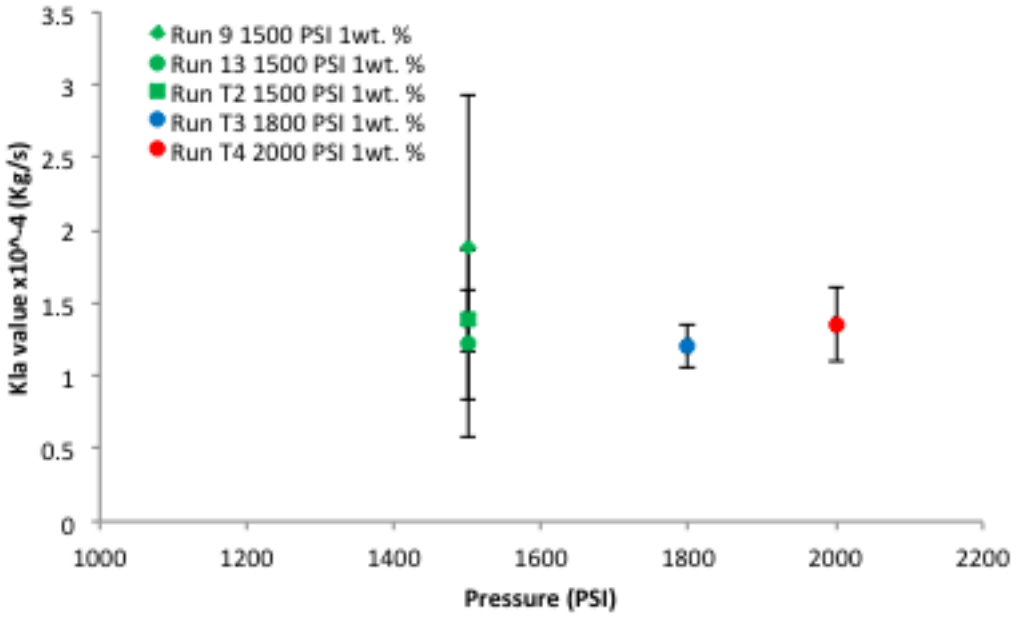

Figure 4.19: The effect of pressure on $K_l a$

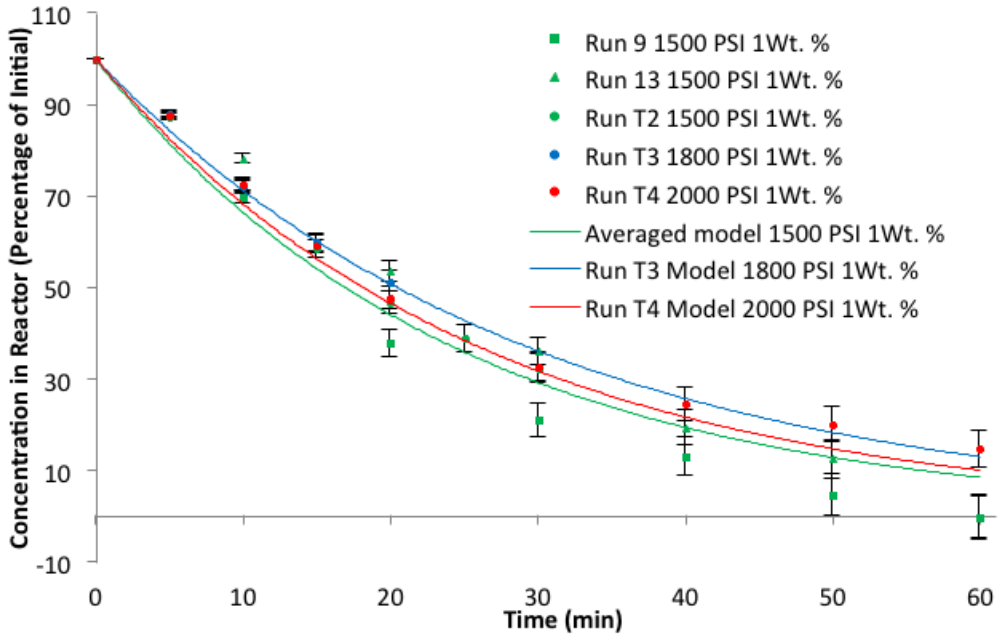

Figure 4.20: Experimental data compared to model trends for pressure change

Although the results collected from varying pressures does not indicate a trend on initial K_la, literature has shown that there is an increasing trend due to increasing pressure. According to Athanassios et al. (1986), it was found that at low pressure from 2.00 MPa (290.1 PSI), the immiscibility, at 40 ˚C, of the ternary system of water, butanol and CO_2 are equal and do not dissolve well together. As the pressure increased, the miscibility of CO_2 increased, while the miscibility of water and $scCO_2$ or butanol did not change.

Tai and Wu (2005) found that surface tension affects interfacial surface area. As the surface tension is lowered, the number of bubbles increases, which increases the interfacial area. They concluded that with an increase in pressure that surface tension decreases, causing more bubbles and an increased interfacial area. However, Tai and Wu also found, as pressure increases the viscosity of the $scCO_2$ will increase, which could lead to a decrease in diffusivity of butanol, causing K_l to decrease. Depending on which parameter is affected the most by pressure (surface tension or viscosity), the initial K_la value could increase, decrease or stay constant. If surface tension is affected the most, the K_la value will increase with pressure, but if viscosity of $scCO_2$ is affected more, the K_la value will decrease. According to the experimental data, the surface tension and viscosity are affected equally, causing no clear increasing or decreasing trend (Tai & Wu, 2005).

4.3.3 The Effects of Mass Flow Rate on $K_l a$

The flow rate of $scCO_2$ of the system was run at 1.26, 3.2 and 9 mL/min, while the rest of the system was kept constant at 1wt.%, 40˚C and a pressure of 1500 PSI. Figure 4.21 shows that the initial $K_l a$ linearly increases as $scCO_2$ flow rate increases. When using the experimental model verse the data collected, it not only represents the data well but also shows that the increased flow rate increases the extracted rate of butanol from water.

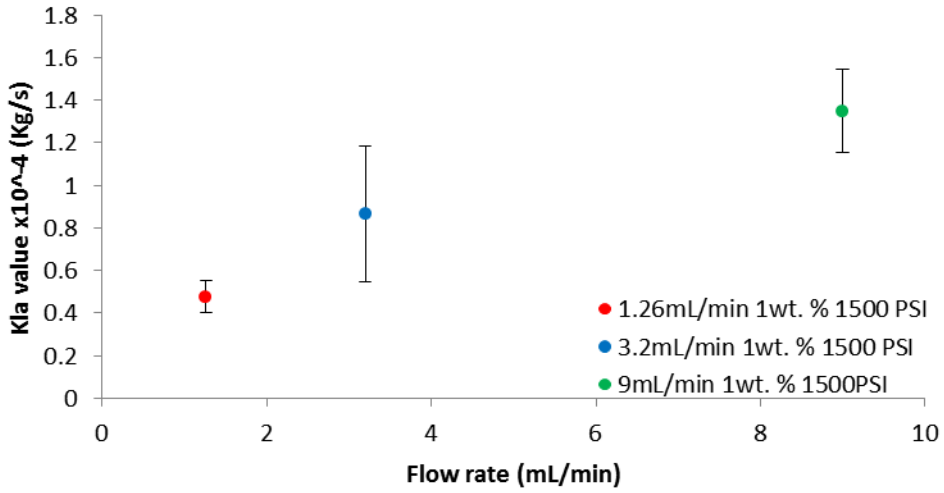

Figure 4.21: The effect of mass flow rate on $K_l a$

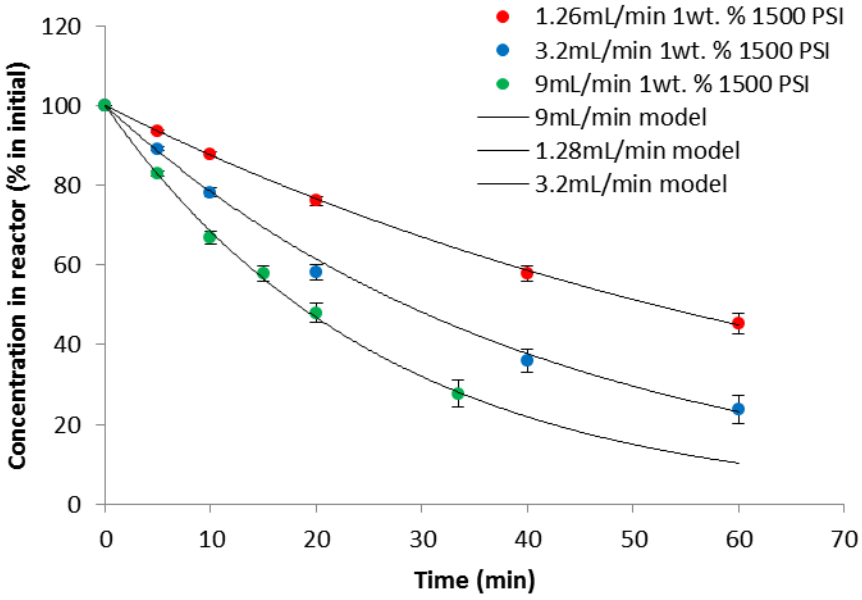

Figure 4.22: Experimental data compared to model trends for mass flow rate change

It is expected for an increase in flow rate to increase the $K_l a$ value and the rate at which butanol is extracted from the reactor because as the flow rate increases, the amount of $scCO_2$ flowing through the reactor increases which creates more bubbles or larger bubbles. These bubbles will have a larger surface area, which will allow for more butanol to be extracted from water at each instance. Although an increased flow rate increases the initial $K_l a$ value and extraction rate of butanol, a cost analysis will have to be done to determine if it's more efficient to use a higher flow rate.

4.4 Theoretical Model Results of Correlations for $K_l a$

The results of the theoretical liquid-liquid extraction model for the butanol reactor were attempting to validate the overall $K_l a$ value of 0.00018 kg/s obtained from the experimental model and it did so with some assumptions.

4.4.1 Calculation for $K_l a$ from K_l and Some Assumptions

The first step of this result was finding K_l correlations that modeled our scenario properly and would produce a $K_l a$ value with an assumed interfacial area that was reasonable. This was done using the three correlations for liquid-liquid mass transfer in Table 4.2 (Cussler, 2009).

Correlation for K_l	Equation	$K_l a$- value (kg/s) *assumed a-value = 0.0007 m^2
(1.1) Large drops – no stirring	(4.1) $\frac{kd}{D} = 0.42\left(\frac{d^3\Delta\rho g}{\rho v^2}\right)^{\frac{1}{3}}\left(\frac{v}{D}\right)^{0.5}$	0.000170
(1.2) Small drops – no stirring	(4.2) $\frac{kd}{D} = 1.13\left(\frac{dv^0}{D}\right)^{0.8}$	0.000162
(1.3) Gas bubbles – stirring	(4.3) $\frac{kd}{D} = 0.13\left(\frac{d^4\left(\frac{P}{V}\right)}{\rho v^2}\right)^{\frac{1}{4}}\left(\frac{v}{D}\right)^{\frac{1}{3}}$	0.000208
Experimental model	–	0.000180

Table 4.2: Comparison of K_l correlations that will be used for theoretical model

It is clear from this chart that the predicted $K_l a$ values from these three correlations are accurate and are within a ~15% error of our experimentally predicted value. This result is good but its overall accuracy is dependent on our assumptions. Each model has a unique variable that is taken into account that changes the way the correlation is affected by the scenario but all of them include the droplet/bubble diameter (d), diffusion coefficient (D), and kinematic viscosity (υ).

The first correlation (1.1) assumes our system has no stirring but that large liquid droplets of supercritical carbon dioxide are rising through the reactor. This correlation includes the density of the $scCO_2$ (ρ) as well as the density difference between the $scCO_2$ and the butanol water mixture ($\Delta\rho$). It also relies more heavily on the viscosity (υ) and diffusion coefficient of the liquid (D). Overall, this correlation was the most accurate within ~5% error of our experimental model prediction.

The second correlation (1.2) makes the same assumptions as the first correlation but it says that the droplets will be a smaller size (< 0.3 cm) and they will behave more like rigid spheres. This correlation is highly dependent on the rising velocity of the droplets (υ^0) and uses this variable as its main driving force for the calculation. In the end, this correlation was within ~10% error of our experimental model.

The third correlation (1.3) assumes a different scenario that treats $scCO_2$ as gas bubbles and includes the effect of stirring. The inclusion of stirring power (P/V) is an important portion of this correlation. This result is within ~15% error from the experimental model and it makes sense that it is the only correlation that predicts a higher $K_l a$ since the bubble shearing would significantly increase interfacial area. However, since our system did include stirring this model is should be most accurate One reason for it not being as accurate is that these models still do not fully represent our system and will over or under predict these values because of it.

4.4.2 Investigating Correlations for the Interfacial Area (a)

The second step to the overall $K_l a$ correlation was to find an interfacial area correlation that could predict the value used in our previous $K_l a$ result and this is what proved the most difficult. For our assumed a-value, in the first step, we used 7 cm^2 as the interfacial area for our calculation. This was done based off estimations that added the

cross sectional area of the reactor and total bubble surface area to determine an estimate for the interfacial area. These values were obtained from taking videos and pictures of a pressurized (1500 PSI) view cell (sight gage) that is located after the pump, to then measure and count the bubble size and quantity. One major problem with this calculation was that the impact of stirring was not fully taken into account, which could have lead to a larger a-value. In order to remedy the shortcomings of this simple calculation, more robust correlations were researched to produce reasonable interfacial area values. Table 4.3 shows the correlations that were used to search for the interfacial area and their results.

Correlation for a	Equation	a- value (m^2)
(2.1) Calculation based	(4.4) $a = \frac{N_{OR}*q}{V_B} * \frac{H_L}{U_B} * \frac{\pi*d_B^2}{A*H_L+N_B V_B}$	226022
(2.2) Video/Picture based	(4.5) $a = \frac{N_{OR}*q}{V_B} * \frac{H_L}{U_B} * \frac{\pi*d_B^2}{A*H_L+N_B V_B}$	995
(2.3) Gas holdup approach	(4.6) $a = \frac{6}{2.5} * \left(\frac{\sigma_L}{\rho_L*g}\right)^{-0.5} * \left(\frac{\mu_L*U_G}{\sigma_L}\right)^{0.25} * \left(\frac{\rho_L*\sigma_L^3}{g*\mu_L^4}\right)^{0.125} * \varepsilon_G$ (4.7) $\varepsilon_G = \frac{U_G}{0.3+2*U_G}$	0.00000015
Assumed a-value	–	0.0007

Table 4.3: Comparison of interfacial area correlations trying to generate assumed a-value

The results of Table 4.3 range from being unreasonably large to fairly close to the assumed a-value but none of them are sufficient in matching the reasonable value we assumed.

The first correlation (2.1) is based off of an area equation that uses separate correlations to determine both the bubble size (d_B) and velocity (U_B) as shown in equations 4.8 and 4.9 (Painmanakul, Wachirasak, Jamnongwong, & Hebrard, 2009).

$$(4.8) \quad d_B = 0.32 * Re^{0.425} * \left(\frac{d_{OR}^2*\sigma}{\Delta\rho*g}\right)^{1/4}$$

$$(4.9) \quad U_B = \frac{\mu_L}{\rho_L*d_B} * (J - 0.857) * M_o^{-0.149}$$

These variables are determined through the Reynolds number for the flow of $scCO_2$ and the dynamic viscosity of the $scCO_2$ as well as its density. All of these factors and equations can be researched further in Painmanakul et al.'s article in the Engineering Journal (Painmanakul et al., 2009). However, at the end of this calculation the result (226022 m^2) was not close to expected value (0.0007 m^2). This could indicate some poor assumptions in the scenario but most likely it is due to the equation not fitting the system we are modeling. To verify that the equation did not fit our system, it was recalculated using variables that were determined without correlations.

The second correlation (2.2) result is the verification of this area correlation not working for our system. Using the same interfacial area correlation, this second result does not calculate bubble size and speed based off of other correlations but rather through video and picture based information. This information is determined through taking videos/photos of a pressurized view cell that is located just before the extraction vessel. From this we are able to use references, such as bolts and measured lengths, to determine bubble size and rising velocity. Overall, this calculation confirmed that this correlation was not suitable for our system as it predicts an area of 995 m^2, which is not feasible in our vessel.

Lastly, the third correlation (2.3) is actually the result of trying multiple combinations of two correlations that were created for the gas holdup and area. This correlation directly relates the gas holdup in our system to the amount of interfacial area that can be present. The full set of correlations consisted of the following equations shown in Table 4.4(Painmanakul et al., 2009).

Eq.	Correlation
a-1	$a = 34.4 * U_G^{0.25} * \varepsilon_G$
a-2	$a = 26.\left(\frac{L_R}{d_R}\right)^{-0.3} (\frac{\rho_L.\sigma_L^3}{g.\mu_L^4})^{-0.003} * \varepsilon_G$
a-3	$a = \frac{6}{2.5}.(\frac{\sigma_L}{\rho_L.g})^{-0.5}.(\frac{\mu_L.U_G}{\sigma_L})^{0.25}.(\frac{\rho_L.\sigma_L^3}{g.\mu_L^4})^{0.125}.\varepsilon_G$
a-4	$a = 4.65 * 10^{-12} * (\frac{U_G}{\mu_L})^{0.51}$
a-5	$a = \frac{6\varepsilon_G}{d_B(1-\varepsilon_G)}$
a-6	$a = 8.54 * U_G^{0.12} * \varepsilon_G$

Eq.	Correlation
εG -1	$\varepsilon_G = \frac{U_G}{0.3 + 2.U_G}$
εG -2	$\varepsilon_G = \frac{U_G}{31 + \beta.(1-e).\sqrt{U_G}}$ $\beta = 4.5 - 3.5.\exp(-0.064.d_B^{1.3})$ $e = -0.18.U_G^{1.8} / \beta$
εG -4	$\varepsilon_G = 0.91.U_G^{1.19} / \sqrt{g.d_B}$

Table 4.4: Full set of correlations used to predict interfacial area from gas holdup

Each combination of the provided correlations in Table 4.4 was tested to determine which interfacial area correlation and gas holdup correlation provided the closest answer to our value. These combinations and results can be seen in Table 4.5.

Correlation	E_g-1	E_g-2	E_g-4
A-1	76.8 m^2	0.356 m^2	1010000 m^2
A-2	13.1 m^2	0.0610 m^2	173000 m^2
A-3	1.50E-07 m^2	6.96E-10 m^2	0.00292 m^2
A-4	1.57E-08 m^2	1.57E-08 m^2	1.57E-08 m^2
A-5	1998 m^2	4.64 m^2	2000 m^2
A-6	8.76 m^2	0.0410 m^2	115000 m^2

Table 4.5: Results of correlation combinations for interfacial area and gas holdup

From this set of results in Table 4.5, the closest answer to our assumed value was using correlations A-3 and E_g-1 to produce 0.00000015 m^2, which is still three orders of

magnitude off from the assumed value. Another observation from these results was that all of these correlations had different dependencies on the gas holdup and various other variables. This gave some correlations more accuracy and the most rigorous interfacial area correlation was also A-3, hence this was chosen as the best option. Ingeneral, the results from Table 4.5 show, , a large range of values from unreasonable to reasonable and from this we demonstate the difficulty in correctly modeling the extraction scenario in a unique system.

The end result for the theoretical model was that there are various correlations to determine the local mass transfer coefficient (K_l) and these can then be applied with a reasonable interfacial area (a) value to produce a $K_l a$ value close to that of the experimental model. However, when operating specific extraction systems that do not match literature based extraction systems it may be difficult to determine an interfacial area value without creating a correlation for the unique system that is being used.

Chapter 5: Conclusions

The scCO2 extraction system was repeatedly run at varying parameters to determine the effects of pressure, initial concentration of butanol, and mass flow rate of supercritical carbon dioxide on the extraction rate and mass transfer coefficient of the system. Standard solutions for the Gas Chromatograph were continuously checked with samples from runs to ensure that the analysis of the samples were consistent. Multiple runs under each condition were completed for validation of results and error analysis was propagated through the analysis of the results. Our conclusions revolve around three things: the running of the experiment, the extraction capabilities of the system, and the models to predict the mass transfer coefficient and predicted extraction rate.

Through running the system over the course of a few months, ways in which to improve the system were found and some implemented. We recommend keeping the heating jacket on the reactor set to 40 ^{o}C while depressurizing to help prevent the carbon dioxide exiting the reactor from freezing over the line. A heating strip was added to the line used to depressurize the system to also help prevent freezing in the line. However, depressurizing the system still takes over 30 minutes to complete and should be completed slowly until below 1000 PSI in the reactor when the carbon dioxide is mostly in gaseous form. In order to prevent loss of butanol from the system we ran sample jars in series to prevent butanol from being vented out of the system. Additionally, to increase mass transfer of butanol from the carbon dioxide stream exiting the reactor to the methanol in the sample jars, diffusers were attached to the lines into the sample jars. The amount of methanol for the later sample jars (past 30 minutes) should be reduced to at least half the normal amount since the amount of butanol extracted is minimal and will be too diluted in a 100g of methanol for the GC to analyze. Due to the limitations of the pump and the extraction rate of butanol we recommend that the system be run for 30 minutes.

The extraction rate of the system was determined as the mass transfer rate of butanol from the aqueous butanol solution to the supercritical carbon dioxide. This was measured via analyzing the butanol collected in the methanol present in the sample jars using the Gas Chromatograph. Throughout the completed runs, approximately 80% of the initial amount of butanol present was extracted in the first 30 minutes of the experiment.

The extraction rate increased when the initial amount of butanol was increased from 1% to 2-3%. The extraction rate of the system for runs with 2 and 3 wt.% were comparable. This may decrease the importance of genetically engineering the organism to survive at 3 wt.% butanol if the extraction rate at 2 wt.% is comparable.

Lastly, the models that were adjusted to fit the system's parameters can be used to predict information about the mass transfer coefficient and extraction rate of the system. The experimental model uses collected data to estimate the initial $K_l a$. The effect of pressure, mass flow rate, and initial concentration on the mass transfer coefficient was analyzed using the experimental model. It was found the initial $K_l a$ experiences slight increase with an increase in concentration. However, since the concentration of butanol decreased with time, the overall $K_l a$ should not be affected by concentration. Through testing pressures ranging from 1500 PSI to 2000 PSI, it was found the initial $K_l a$ was not impacted with a change in pressure. We believe that the range of pressures tested was not significant enough to impact the mass transfer coefficient, but the system could not be run at much higher of a pressure. Increasing the mass flow rate of the supercritical carbon dioxide solvent from 1.26 to 9 mL/min caused the $K_l a$ of the system to increase. This result makes sense since an increase in the flow of the solvent through the aqueous butanol solution would increase the amount of surface area and therefore should help improve the mass transfer rate.

The theoretical model was created to validate the experimentally determined $K_l a$. When assuming a realistic interfacial surface area, three different theoretical models for $K_l a$ were found to be around the experimental $K_l a$ value, validating the experimental $K_l a$ value. Then the experimental $K_l a$ value was used in the same experimental model to predict extraction results at various pressures, initial concentrations, and mass flow rates. When overlaying predicted trends created by the model with experimental data at various conditions, the trends accurately imposed on the data points. Therefore, we conclude that adjusting Tai and Wu's model from an ethanol extraction system to a butanol extraction system with supercritical carbon dioxide, it can accurately predict extraction results and the mass transfer coefficient of our system. This model can be used to predict extraction results at conditions that have not yet been tested on the system.

Chapter 6: Recommendations and Future Work

After completing our project, our team has a few recommendations for operation of the system, the next steps for research, and safety improvements of the system in the future. With regards to the operation of the system, we recommend to run the extraction unit in 30-minute intervals. We found that in the first 30 minutes, 80% of the total amount of butanol in the system was extracted. In 60 minutes, close to 100% of butanol can be extracted, however we believe it is more efficient to obtain 80% of butanol in 30 minutes rather than 100% in double the amount of time.

In addition, we have a few recommendations for the next steps of research to reach the end goal of efficiently extracting alcohols with the organism residing in the system. To start off, the system should be tested with all appropriate alcohols besides butanol, produced by *B. Megaterium*. This will provide predictions for the extraction rates of all potential types of alcohol. After all alcohols are tested in the system, the organism can be introduced in a semi-batch mode. A semi-batch mode is recommended because we believe it would be the most effective set-up when considering economics and safety. Once data is obtained for the semi-batch mode containing organisms, the experimental and theoretical models our team developed can be modified to incorporate any affects the organism may have on extraction results. Lastly, the theoretical model for interfacial area (a) should be further investigated to increase the accuracy of the theoretical model. This can be done by finding a correlation for interfacial area (a) that accurately represents the parameters of our system.

To improve the safety of the systems operation we recommend developing a safer method to depressurize the system. The ideal method would take a shorter amount of time and would not run the risk of freezing the line through which the system is depressurized. To add to this, our team recommends that the plastic shields surrounding the system remain on throughout the entirety of every run to protect the researchers. We also recommend a replacement of plastic tubes connecting the collection jars with a material that can withstand higher temperatures. This will allow the use of heating tape on the lines connecting the sample jars. The heating tape would reduce the possibility of the buildup of pressure from the lines freezing over. Lastly, the team recommends the use of double layer

Pyrex glass collection jars to reduce the potential of shattering and explosion if there is a buildup of pressure within the collection vessels.

References

Biobutanol. (2015). *Emerging Fuels.* Retrieved December 04, 2015, 2015

Butamax. (2016). from http://www.butamax.com/

Carbon cycle 2.0. (ND). *Biofuels.* Retrieved November 6, 2015, from http://carboncycle2.lbl.gov/research/focus-areas/biofuels/

Chen, H.-I., Chang, H.-Y., & Chen, P.-H. (2002). High-pressure phase equilibria of carbon dioxide + 1-butanol, and carbon dioxide + water + 1-butanol systems. *Journal of Chemical and Engineering Data, 47*(4), 776-780. doi: 10.1021/je010237q

Clark, D. S., & Blanch, H. W. (1997). *Biochemical Engineering* (Second ed.): CRC Press.

Cussler, E. (2009). *Diffusion: Mass transfer in fluid systems* (3rd ed.). New York: Cambridge University Press.

Delgado, B., & Pessoa, F. L. P. (2014). Simulation of butanol production by an integrated fermentation process using supercritical fluid extraction with carbon dioxide. *New Biotechnology, 31, Supplement*, S116. doi: http://dx.doi.org/10.1016/j.nbt.2014.05.1893

Earley, J., & McKeown, A. (2009). *Red, white, and green : transforming U.S. biofuels*. Washington, D.C.: Worldwatch Institute.

Energy Explained. (2015). Retrieved December 04, 2015, 2015

Ethanol as a Transportation Fuel. (ND). Retrieved October 28, 2015, 2015, from http://www.consumerenergycenter.org/transportation/afvs/ethanol.html

Ezeji, T. C., Qureshi, N., & Blaschek, H. P. (2007). Bioproduction of butanol from biomass: from genes to bioreactors. *Current opinion in biotechnology, 18*(3), 220-227.

Fortman, J. L., Chhabra, S., Mukhopadhyay, A., Chou, H., Lee, T. S., Steen, E., & Keasling, J. D. (2008). Biofuel alternatives to ethanol: pumping the microbial well. *Trends in biotechnology, 26*(7), 375-381.

The Freezing Point And The Dew Point – Part 2. (2010). Retrieved 4/26/2016, from https://stevengoddard.wordpress.com/2010/09/05/the-freezing-point-and-the-dew%C2%A0point-part-2/

Gevo. (2016). from http://www.gevo.com/

Herrero, M., Mendiola, J. A., Cifuentes, A., & Ibáñez, E. (2010). Supercritical fluid extraction: Recent advances and applications. *Journal of Chromatography A, 1217*(16), 2495-2511. doi: http://dx.doi.org/10.1016/j.chroma.2009.12.019

How we use energy (2015). from http://www.eia.gov/energyexplained/index.cfm?page=us_energy_use

Laitinen, A., & Kaunisto, J. (1999a). Oldshue-Rushton Column in Supercritical Fluid Extraction. *Separation Science and Technology, 34*(9), 1859-1872. doi: 10.1081/SS-100100743

Laitinen, A., & Kaunisto, J. (1999b). Supercritical fluid extraction of 1-butanol from aqueous solutions. *The Journal of Supercritical Fluids, 15*(3), 245-252. doi: 10.1016/S0896-8446(99)00011-X

McHugh, M. A., Krukonis, V. J., Knovel, O., Gas Engineering Library - Academic, C., Knovel, C., & Chemical Engineering Library - Academic, C. (1994). *Supercritical fluid extraction: principles and practice* (Vol. 2nd). Boston: Butterworth-Heinemann.

Moreno, T., Tallon, S. J., & Catchpole, O. J. (2014). Supercritical CO2 Extraction of 1 ‐ Butanol and Acetone from Aqueous Solutions Using a Hollow ‐ Fiber Membrane Contactor. *Chemical Engineering & Technology, 37*(11), 1861-1872. doi: 10.1002/ceat.201300700

Odell, P. R. (1999). Non-renewable energy sources. *Energia (Roma), 20*(2), 20-25.

Oudshoorn, A., Van Der Wielen, L. A. M., & Straathof, A. J. J. (2009). Assessment of options for selective 1-butanol recovery from aqueous solution. *Industrial and Engineering Chemistry Research, 48*(15), 7325-7336. doi: 10.1021/ie900537w

Özkal, S. G., Salgın, U., & Yener, M. E. (2005). Supercritical carbon dioxide extraction of hazelnut oil. *Journal of Food Engineering, 69*(2), 217-223. doi: http://dx.doi.org/10.1016/j.jfoodeng.2004.07.020

Painmanakul, P., Wachirasak, J., Jamnongwong, M., & Hebrard, G. (2009). Theoretical Prediction of Volumetric Mass Transfer Coefficient ($K_l a$) for Designing and Aeration Tank. *Engineering Journal, 13*(3). Retrieved from

Panagiotopoulos, A. Z., & Reid, R. C. (1986). Multiphase High Pressure Equilibria In Ternary Aqueous Systems. *Fluid Phase Equilibria, 29*(C), 525-534. doi: 10.1016/0378-3812(86)85051-8

Peet, K. C., Freedman, A. J. E., Hernandez, H. H., Britto, V., Boreham, C., Ajo-Franklin, J. B., & Thompson, J. R. (2015). Microbial growth under supercritical CO2. *Applied and environmental microbiology, 81*(8), 2881-2892. doi: 10.1128/AEM.03162-14

Qureshi, N. (2010). Agricultural residues and energy crops as potentially economical and novel substrates for microbial production of butanol (a biofuel). *Plant Sci. Rev, 249*.

Rahimi, E., Prado, J. M., Zahedi, G., & Meireles, M. A. A. (2011). Chamomile extraction with supercritical carbon dioxide: Mathematical modeling and optimization. *The Journal of Supercritical Fluids, 56*(1), 80-88. doi: 10.1016/j.supflu.2010.11.008

Rosa, P. T. V., & Meireles, M. A. A. (2005). Rapid estimation of the manufacturing cost of extracts obtained by supercritical fluid extraction. *Journal of Food Engineering, 67*(1), 235-240. doi: 10.1016/j.jfoodeng.2004.05.064

Seader, J. D., & Henley, E. J. (1998). Supercritical-Fluid Extraction *Separation Process Principles* (pp. 641-651). New York: John Wiley & Sons, Inc.

Sigma-Aldrich. (2015a). *1-Butanol*.

Sigma-Aldrich. (2015b). *Methanol*.

Tai, C. Y., & Wu, S.-Y. (2005). Kinetics of supercritcal fluid extraction of ethanol from aqueous solution. *Chemical Engineering Communications, 192*(10), 14.

Thompson, J., Prather, K., & Timko, M. (2014). *Systems Biology Towards a Continuous Platform for Biofuels Production*. Submitted proposal to DOE. U.S. Department of Energy. Massachusetts Institute of Technology

Worcester Polytechnic Institute. n/a.

Vázquez da Silva, M., Barbosa, D., & Ferreira, P. O. (2002). High pressure vapor-liquid equilibrium data for the system carbon dioxide + decanal at 288.2, 303.2, and 313.2 K. *Journal of Chemical and Engineering Data, 47*(5), 1171-1172. doi: 10.1021/je020009b

Wade, L. G., & Simek, J. W. (2011). *Organic Chemistry, 8th Edition*.

Worrest, A. N., Fletcher, B. J., & Timko, M. T. (2015). *Modeling the Thermodynamics of Biobutanol Extraction Using scCO2 Solvent*. Worcester, MA U6 - ctx_ver=Z39.88-

2004&ctx_enc=info%3Aofi%2Fenc%3AUTF-8&rfr_id=info:sid/summon.serialssolutions.com&rft_val_fmt=info:ofi/fmt:kev:mtx:book&rft.genre=book&rft.title=Modeling+the+Thermodynamics+of+Biobutanol+Extraction+Using+scCO2+Solvent&rft.au=Worrest%2C+Alan+Nathan+Student+author+--+CM&rft.au=Fletcher%2C+Benjamin+Joseph+Student+author+--+CM&rft.au=Timko%2C+Michael+T.%2C+Faculty+advisor+--+CM&rft.date=2015-01-01&rft.pub=Worcester+Polytechnic+Institute&rft.externalDocID=2891026&paramdict=en-US U7 - eBook: Worcester Polytechnic Institute.

Appendix A: Start up, Running, and Shut Down Procedure

1. Turn chiller on and set to 0°C (45 mins to cool to target temperature)
2. Power switch is in the back and controller
3. Check cooling fluid has enough liquid
4. Fill methanol collection vials (large vials: 100 grams, small vials: 50 grams) and hook up the vials in series to the exit stream of system.
5. Record exact weights of the empty vials and the vials containing methanol before hooking up to system for collection.
6. Fill reactor vessel with butanol/water solution, measure concentrations (1-3 wt%), *MAKE SURE VESSEL LINES ARE CLOSED (valve below vessel should be perpendicular to line)
7. Attach reactor vessel to system with clamps
8. Check O-RING before/after each run
9. Wires connected to the reactor unit should point towards the sugar water vessel (towards the back right side of the system when looking from the front side) - this makes it easier to secure the heating jacket
10. Tighten nut above valve (use fingers first to make sure the thread isn't slipping)
11. Wrap heating jacket around vessel - tie strings
12. Turn heating jacket (40°C) and heating line tapes (60°C) on. Put stirrer on (flip motor switch to III).
13. Turn on CO_2, watch leftmost gauge (pressure of tank - should stay at about 900PSI)
14. Around back, turn valve for CO_2 open slightly to purge line, for about 5 seconds. (wait for gurgle sound in line) Close valve after purge step is complete.
15. Open the two valves below the reactor and the value at the top of the reactor.
16. Turn on the pumps (Watch for bubbles in the view cell. Middle gauge needle should tick with sounds).
17. Wait for pressure to reach 1500 PSI on the main pressure gauge above reactor and start timer for run when a substantial stream of gas is flowing through the methanol filled collection vessels. Now use Wet test meter to monitor the gas flow rate during the run.
18. Switch samples every (10-15) minutes. *CHECK FOR FROZEN PIPES (could cause surging in the exit stream)

Shut off (Emergency):

1. Turn off pumps to stop build up of pressure
2. Turn off CO_2 supply
3. Depressurize the column.
4. There are two valves connected to the reactor that are used for depressurization. Use the one with the attached metal pipe to collect any exiting fluid in a sampling container near base of system.
5. ***Release pressure very slowly. If gas is released too quickly, the pipes will freeze over, causing blockages. Change valve release point when first valve snows over and no fluid is exiting system.

Appendix B: GC vial preparation

Results Analysis Setup:

1. All sample containers should be weighed before running the experiment and should then be weighed after collection and recorded. The two sample jars in each series should be added together before recording their weight.
2. After weighing the sample containers and combining the liquid from the series jars, a portion of the sample will be transferred to a vial (5 dram) and then the containers will be emptied into waste containers.
3. The sample containers will then be washed and prepared for another collection interval for the system.
4. The collected sample portion in the vial (5 dram) will then be transferred to a GC vial for analysis.
5. All vials will be labeled for storage in a refrigerator until analysis can be performed.
6. GC analysis will be be performed and resulting data collected.